

AD-A058 679

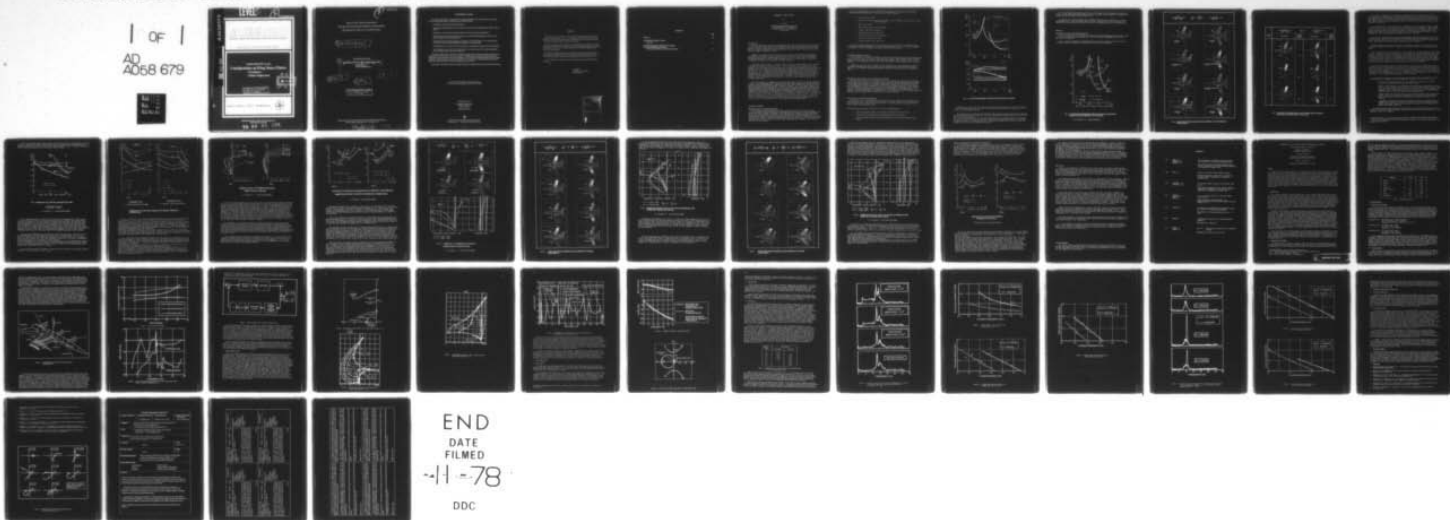
ADVISORY GROUP FOR AEROSPACE RESEARCH AND DEVELOPMENT--ETC F/G 1/1  
CONSIDERATIONS ON WING STORES FLUTTER ASYMMETRY, FLUTTER SUPPRE--ETC(U)  
JUL 78

UNCLASSIFIED

AGARD-R-668

NL

1 of 1  
AD  
A058 679



AD A0 58679

LEVEL II

5 SC AGARD-R-668

# AGARD

ADVISORY GROUP FOR AEROSPACE RESEARCH & DEVELOPMENT

7 RUE ANCELLE 92200 NEUILLY SUR SEINE FRANCE

DDC FILE COPY

AGARD REPORT No. 668

## Considerations on Wing Stores Flutter

- Asymmetry
- Flutter Suppression

DDC  
 15 19  
 F

This document has been approved  
 for public release and sale; its  
 distribution is unlimited.

NORTH ATLANTIC TREATY ORGANIZATION



DISTRIBUTION AND AVAILABILITY ON BACK COVER

78 09 14 062

5

NORTH ATLANTIC TREATY ORGANIZATION  
ADVISORY GROUP FOR AEROSPACE RESEARCH AND DEVELOPMENT  
(ORGANISATION DU TRAITE DE L'ATLANTIQUE NORD)

14 AGARD-R-668

6 AGARD Report No.668  
CONSIDERATIONS ON WING STORES FLUTTER  
- Asymmetry  
- Flutter Suppression

D D C  
RECEIVED  
SEP 15 1978  
F

11 Jul 78

12 44 p.

This document has been approved for public release and sale; its distribution is unlimited.

Papers presented at the 46th Structures and Materials Panel Meeting, held at Aalborg, Denmark, 10-14 April 1978.

78 09 14 062  
400 043

alt

## THE MISSION OF AGARD

The mission of AGARD is to bring together the leading personalities of the NATO nations in the fields of science and technology relating to aerospace for the following purposes:

- Exchanging of scientific and technical information;
- Continuously stimulating advances in the aerospace sciences relevant to strengthening the common defence posture;
- Improving the co-operation among member nations in aerospace research and development;
- Providing scientific and technical advice and assistance to the North Atlantic Military Committee in the field of aerospace research and development;
- Rendering scientific and technical assistance, as requested, to other NATO bodies and to member nations in connection with research and development problems in the aerospace field;
- Providing assistance to member nations for the purpose of increasing their scientific and technical potential;
- Recommending effective ways for the member nations to use their research and development capabilities for the common benefit of the NATO community.

The highest authority within AGARD is the National Delegates Board consisting of officially appointed senior representatives from each member nation. The mission of AGARD is carried out through the Panels which are composed of experts appointed by the National Delegates, the Consultant and Exchange Program and the Aerospace Applications Studies Program. The results of AGARD work are reported to the member nations and the NATO Authorities through the AGARD series of publications of which this is one.

Participation in AGARD activities is by invitation only and is normally limited to citizens of the NATO nations.

The content of this publication has been reproduced  
directly from material supplied by AGARD or the authors.

Published July 1978

Copyright © AGARD 1978  
All Rights Reserved

ISBN 92-835-1290-1



*Printed by Technical Editing and Reproduction Ltd  
Harford House, 7-9 Charlotte St, London, W1P 1HD*

PREFACE

↓  
Air Forces in many countries have to face problems of aeroelasticity and flutter with aircraft carrying more and more stores. The two papers of this Report presented to the Sub-Committee on Aeroelasticity of the Structures and Materials Panel during the 46th Meeting of the Panel deal with two different aspects of the problem.

— The paper of A. Lotze is concerned with the many configurations, symmetric or asymmetric, that may occur and with their consequences on the natural modes of the structure. It clarifies the difficulties one has to face to clear the flight domain for all flight configurations and proposes useful approaches.

— The paper of C. Hwang, B. A. Winther, T. E. Noll and M. G. Farmer deals with the difficult problem of flutter suppression; it exposes the approach, the design, and the wind tunnel tests of the model of a fighter, carrying stores and equipped with a flutter suppression device.

The two papers are of great interest to aeroelasticians and may give useful help to the designer.  
↑

G. COUPRY  
Chairman, Sub-Committee  
on Aeroelasticity

ACCESSION for	
RTIS	White Section <input checked="" type="checkbox"/>
DDC	Buff Section <input type="checkbox"/>
UNANNOUNCED	<input type="checkbox"/>
JUSTIFICATION	
BY	
DISTRIBUTION/AVAILABILITY CODES	
Doc.	SPECIAL
A	

**CONTENTS**

	<b>Page</b>
<b>PREFACE</b>	iii
<b>ASYMMETRIC STORE FLUTTER</b> by A.Lotze	1
<b>DEMONSTRATION OF AIRCRAFT WING/STORE FLUTTER SUPPRESSION SYSTEMS</b> by C.Hwang, B.A.Winther, T.E.Noll and M.G.Farmer	21

# ASYMMETRIC STORE FLUTTER

by

A. Lotze

MESSERSCHMITT-BÖLKOW-BLOHM GmbH.  
Unternehmensbereich Flugzeuge  
Postfach 801160 - 8 München 80  
W.-Germany

## INTRODUCTION

Numerous missions of military aircrafts are dealing with asymmetrical store configurations. External stores may be flown asymmetrically throughout the whole mission like electronic pods, camera pods and pylon mounted fuel tanks in combination with external weapon carriage. Asymmetrical store configurations also can occur temporarily by asymmetrical sequences of weapon release.

Asymmetrical effects generated by tolerances in mass and stiffness distributions are generally expected to be less important for flutter, but may create considerable problems during ground resonance and flight flutter tests. Caused by closely spaced frequencies, beating of resonance mode frequencies can arise which makes it difficult to identify the mode and to evaluate the exact damping.

Performing flutter work it is quite common to base the investigation on the assumption that the flutter condition is more difficult to achieve for asymmetrical configurations. Therefore a procedure often used to reduce the size of the flutter presentation task is to analyze all configurations as being carried symmetrically [1], [2], [3]. Beyond this, in his paper on "Flutter of Aircraft with External Stores", presented at the U.S. Air Force Aircraft/Stores Compatibility Symposium in 1969, H. Katz indicated the possibility to increase the flutter speed of store configurations by "built-in" unsymmetries like making the left-hand pylon of different stiffness than the right-hand pylon. Of course this procedure would only be reliable if for a given aircraft all possible store configurations are proved to flutter at higher speeds when the system is made asymmetrical.

First indications of asymmetrical store instabilities at lower air speeds than measured for the related symmetrical configurations were found during wind tunnel testing of a model, having sweepable wings. Results of this test were presented at the "Specialists Meeting on Wing-With-Stores Flutter" in Munich 1974 [4]. Due to the small damping gradients measured for the asymmetrical store configurations, the determination of the exact flutter speed was difficult and still uncertainties remained whether the measurements demonstrate real flutter or rather have to be explained by forced vibrations caused by marginally stable modes. In the meantime a large number of asymmetrical store configurations have been investigated by analysis and further wind tunnel testing to establish the physical background for the flutter mechanism of asymmetrical stores and to find out whether unfavourable effects of asymmetries exist only for mild flutter or could also occur for flutter cases, exhibiting large gradients of aerodynamic damping with air-speed. Results of this asymmetrical store study will be presented here.

## TECHNICAL APPROACH

### Representation of Aircraft Structure

The aircraft investigated here features sweepable wings which require single point attachments for the inboard and outboard wing pylons. Due to this requirement the values for the attachment stiffness in the yaw degree of freedom are relatively small for the wing and also for the pylons. The flexibilities of the attachments had to be considered by special degrees of freedom in roll, pitch and yaw for the wing and in yaw for the pylon. Since it was proved by analysis that the flexibility of fin, taileron and fuselage has no effect on store flutter, these components were assumed to be rigid for most of the calculations.

For the representation of wing-external store dynamics the following generalized coordinates were introduced into vibration and flutter analyses.

- . 3 Rigid aircraft modes
- . 4 Elastic wing modes (first and second vertical bending, first torsion, first lateral bending)
- . 3 Wing pivot modes
- . 3 Wing inboard store junction modes
- . 3 Elastic inboard pylon modes
- . 1 Inboard pylon pivot (yaw) mode
- . 3 Wing outboard store junction modes
- . 3 Elastic outboard pylon modes
- . 1 Outboard pylon pivot (yaw) mode

Using the Q-R Algorithmus, the flutter equation was solved for the equivalent amount of structural damping  $g$ , necessary to provide harmonical oscillations. Structural damping as measured in ground resonance tests has not been considered here.

#### Unsteady Aerodynamic Forces

Three-dimensional unsteady aerodynamic forces were calculated for the wing using kernel function theories [5]. According to the operational speed of most external store configurations, the calculations in general have been performed for the subsonic region at Mach number 0.9. For comparison with flutter model test results some calculations are based on  $M = 0.3$ .

Investigations show that in most cases the influence on flutter behaviour caused by unsteady aerodynamic forces on external stores and store-wing interference effects is small [6],[7]. Therefore unsteady aerodynamic effects of the store are not considered here.

#### Mathematical Description of the Asymmetrical System

The dynamical behaviour of the symmetrical clean aircraft was described by available symmetrical and antisymmetrical component modes. Asymmetrical external stores were added to the symmetrical aircraft by coupling asymmetrical store modes (representing the mass and stiffness distribution of individual pylon-store systems on each side of the wing) with the symmetrical and antisymmetrical clean aircraft modes dynamically. This approach has the advantage of using proved structural and aerodynamical representations of the aircraft, already established for symmetrical and antisymmetrical investigations. Having defined a set of symmetrical and antisymmetrical clean aircraft modes and asymmetrical store modes, the vibration and flutter equations can be solved as usual.

#### Description of the Flutter Mechanism

The mechanism of the symmetrical and asymmetrical store flutter on principle can be demonstrated by Fig. 1 which shows the variation of flutter speed and modal frequencies with increasing store radius of gyration for the store pitch axis as resulted from the flutter model test mentioned above.

The three important modes involved in the flutter mechanism are:

- . First wing bending mode with in-phase lateral motion of the store
- . Store pitch mode exhibiting large amplitudes of wing torsion
- . Store roll mode coupling with wing bending and out-of-phase lateral store motion



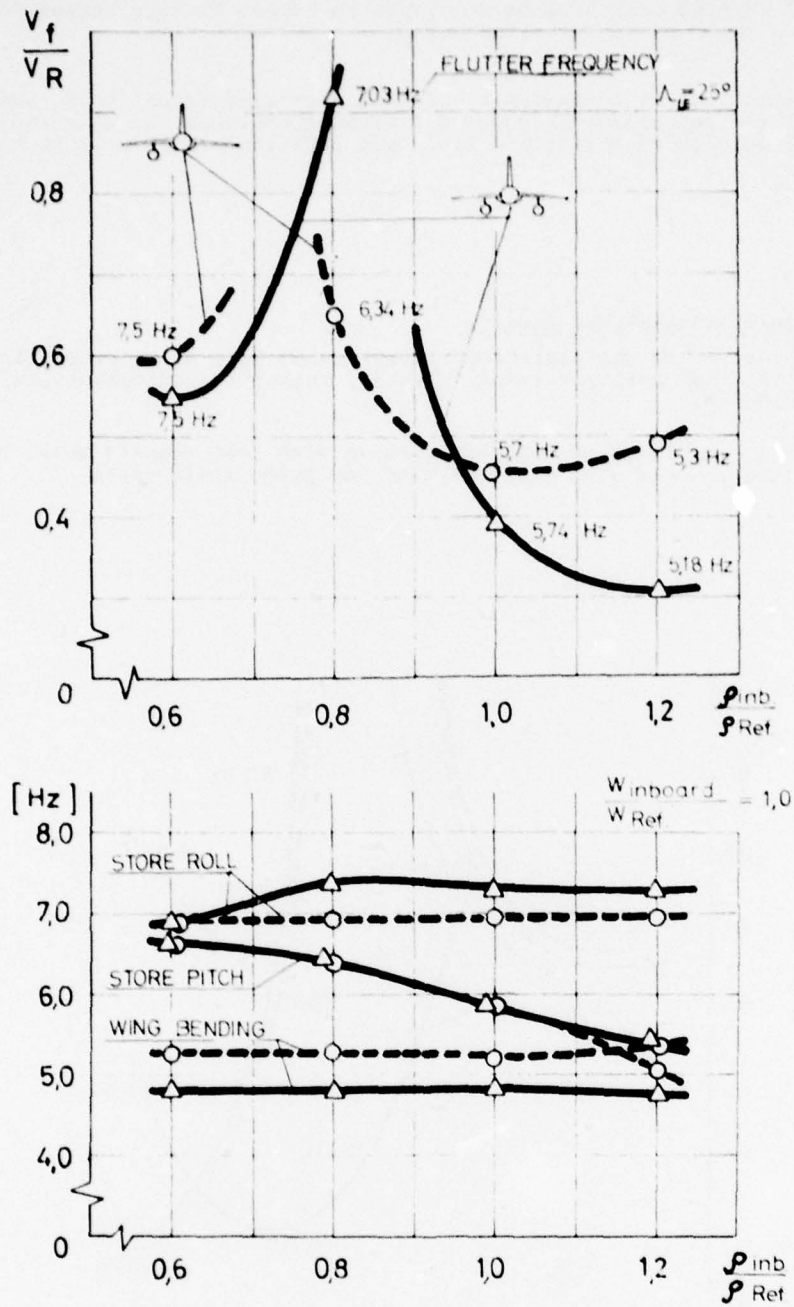


FIG. 1 FLUTTER SPEED AND MODAL FREQUENCIES VERSUS RADIUS OF GYRATION

Frequencies of the store roll mode and wing bending mode are not affected by variation of the pitch inertia, but the distances to the store pitch frequency are reduced if the store is carried asymmetrically.

The diagram on top indicates two different flutter modes characterized by the coupling of store pitch with wing bending for the right-hand branch and store pitch with store roll for the left-hand branch. Due to the increased frequency of the wing bending mode for asymmetrical store carriage the value for the pitch inertia related to the minimum flutter speed condition is shifted to smaller values of  $\rho$ , thus creating the capability of asymmetrical flutter at lower air speeds in the range of intermediate values of  $\rho$ .

For the stiffness and mass distributions investigated by this diagram, the pitch-roll flutter of the left-hand branch seems to result to higher flutter speeds for asymmetrical stores inside the range of actual values of  $\phi$ .

To confirm this flutter mechanism as deduced from wind tunnel tests and to examine the asymmetrical flutter behaviour under different conditions for wing and pylon stiffnesses and store weights, an analytical study was initiated which will be discussed now.

## RESULTS

### Correlation of Test and Analysis Results

For all external store configurations investigated here, symmetrical flutter was found to be more critical than antisymmetrical flutter. Therefore antisymmetrical flutter will not be considered.

Fig. 2 shows a comparison of analysis results with test results which have been obtained by the flutter model with modified wing and pylon stiffnesses.

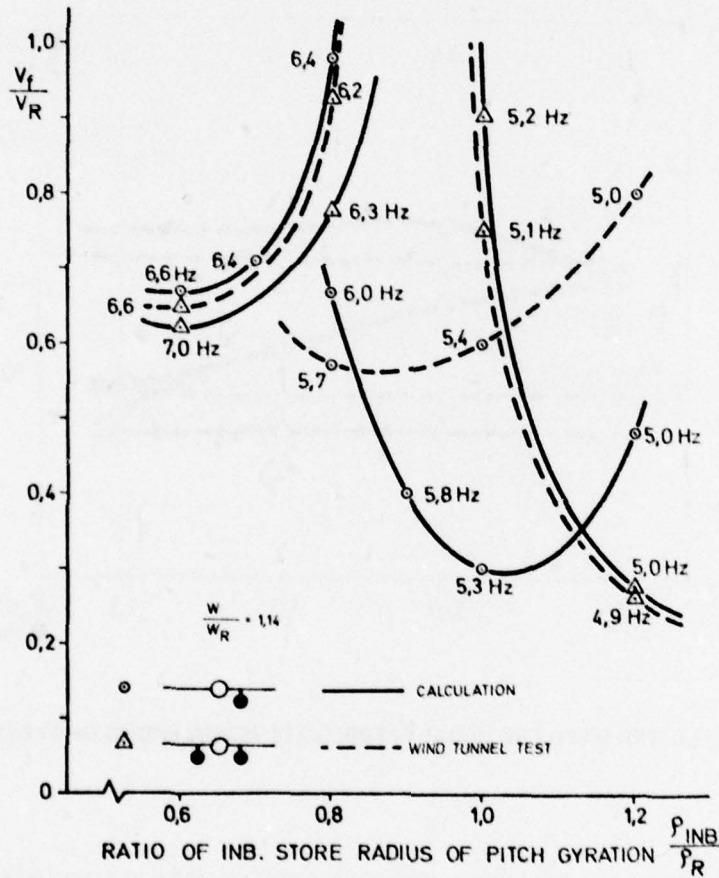
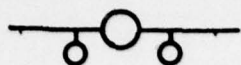
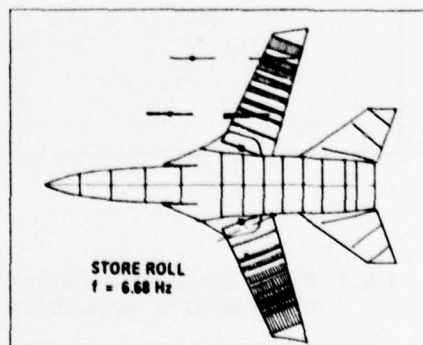
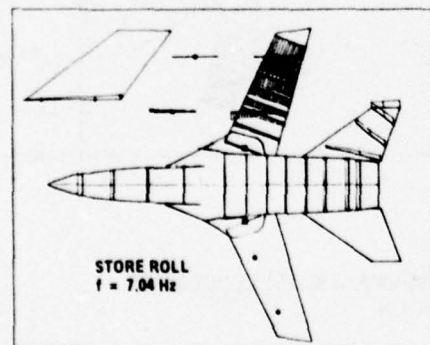
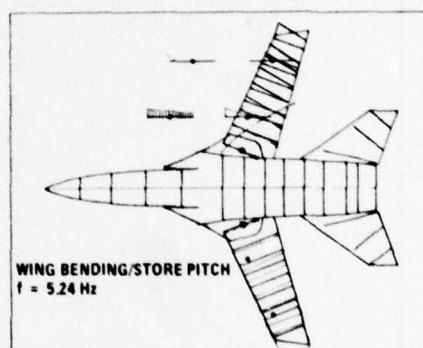
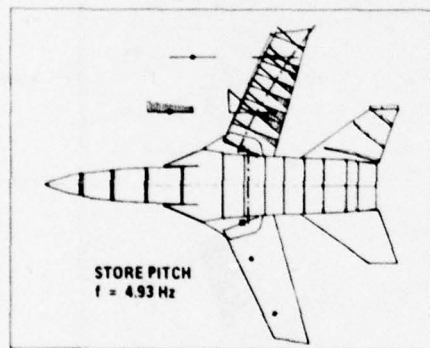
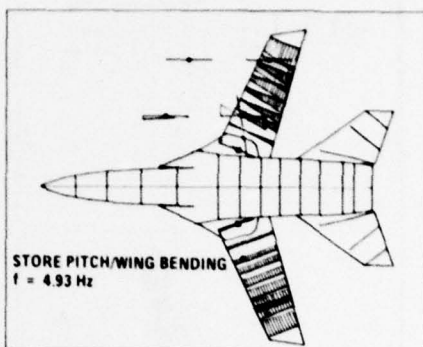
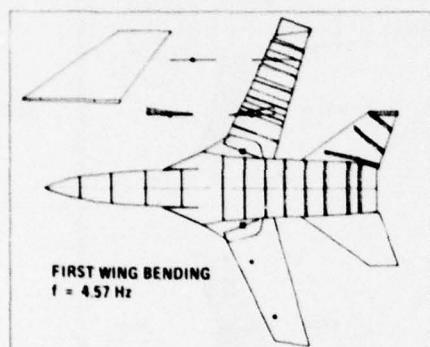
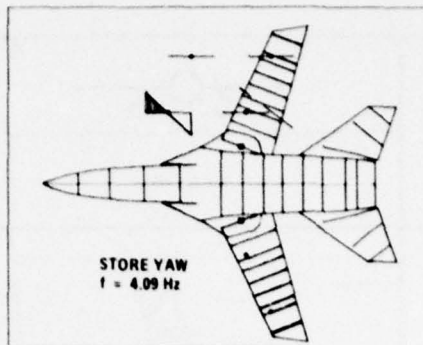
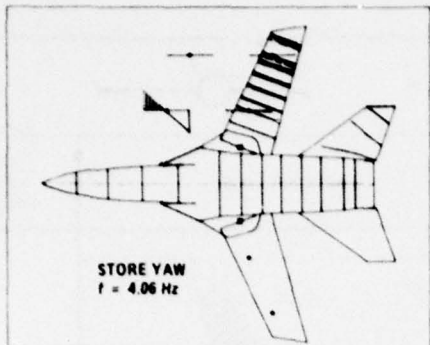
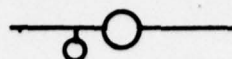


FIG. 2 FLUTTER SPEED VERSUS INBOARD STORE PITCH RADIUS OF GYRATION FOR SYMMETRICAL AND ASYMMETRICAL CONFIGURATIONS

M = 0.3, DRY WING,  $\lambda = 25'$ , NOMINAL PYLON STIFFNESS



$$\frac{W}{W_{REF}} = 1.0 \quad \frac{P_{PITCH}}{P_{REF}} = 1.2$$



**FIG. 3 INBOARD STORE NORMAL MODE SHAPES FOR SYMMETRICAL AND ASYMMETRICAL STORE CARRIAGE**

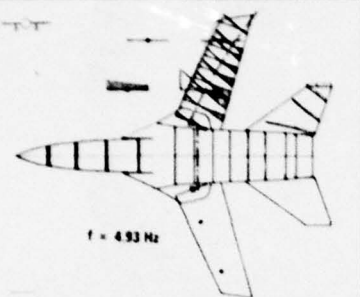
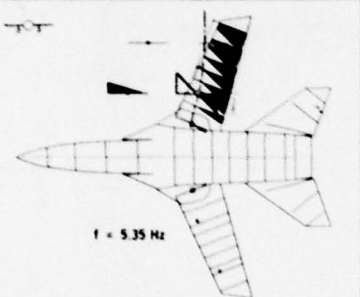
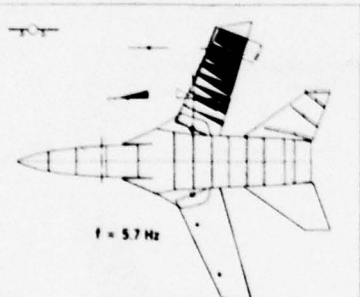
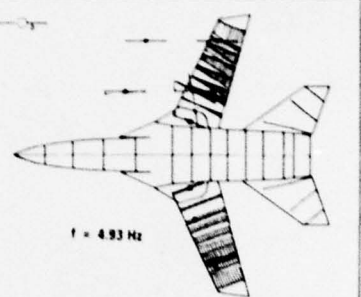
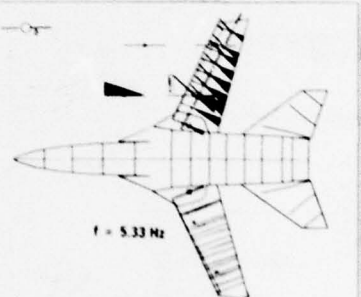
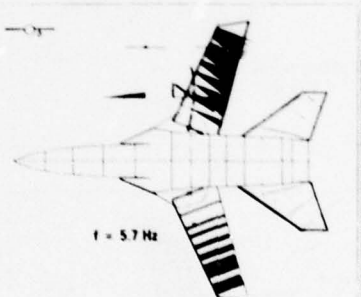
$\frac{P_{PITCH}}{P_{REF}}$	$\frac{W}{W_{REF}} = 1.14$	
	STORE PITCH MODE	FIRST WING BENDING FREQUENCY
1.2	 <p><math>f = 4.93 \text{ Hz}</math></p>	4.57 Hz
1.0	 <p><math>f = 5.35 \text{ Hz}</math></p>	4.53 Hz
0.8	 <p><math>f = 5.7 \text{ Hz}</math></p>	4.57 Hz
	STORE PITCH MODE	FIRST WING BENDING FREQUENCY
	 <p><math>f = 4.93 \text{ Hz}</math></p>	5.24 Hz
	 <p><math>f = 5.33 \text{ Hz}</math></p>	5.16 Hz
	 <p><math>f = 5.7 \text{ Hz}</math></p>	5.1 Hz

FIG. 4 VARIATION OF PITCH MODE NODAL LINE AND NORMAL MODE FREQUENCIES WITH RADIUS OF INBOARD STORE PITCH GYRATION

In general the mechanism of flutter as found during earlier wind tunnel testing are confirmed. For symmetrical store configurations the two different branches of flutter are separated well and agreement between test and analysis is satisfactory, considering that small differences between structural model data and design data can effect the minimum flutter speed to occur at smaller values of  $\rho$ , thus shifting the whole curve as indicated by the diagram.

As it turned out for the configurations considered in this figure, the damping gradient in the flutter point was very small for asymmetrical stores at  $\rho/\rho_{Ref.}$  values between 1.2 and 0.8. This made it extremely difficult to define the exact flutter speed by model testing which may explain the difference between measured and calculated results for asymmetrical stores. Nevertheless calculations and also measurements indicate a range of possibly lower flutter speed for asymmetrical store carriage.

For the left-hand branch no results are available from test for asymmetrical store configurations. Calculated differences between symmetrical and asymmetrical stores seems to be less essential, but, as it will be shown later, this behaviour could be changed for other combinations of wing and pylon stiffnesses and store weights.

Whether asymmetrical store carriage will increase or reduce the flutter speed can already be deduced from changes of frequencies and mode shapes of corresponding normal modes.

Fig. 3 demonstrates the differences in mode shapes for the modes important for store flutter, depicting a value of store pitch inertia close to the minimum flutter speed condition for symmetrical stores. Whereas for the symmetrical configuration the pitch mode exhibits large wing torsional displacements, being able to generate severe flutter, the contribution of wing torsion to the asymmetrical store pitch mode is small. The asymmetrical store pitch frequency is shifted below the wing bending frequency which leads to a mild flutter case. The store yaw and store roll modes in both cases are well separated from the store pitch mode and are not involved in the flutter mechanism.

How the wing bending frequency and the shape of the store pitch mode change with varying  $\rho$ -value is shown by Fig. 4. This figure illustrates for the symmetrical configuration the tuning of frequency between store pitch and wing bending and the variation of the pitch nodal line from the most critical position at  $\rho/\rho_{Ref.} = 1.2$  to a less critical forward position at  $\rho/\rho_{Ref.} = 0.8$ . For the asymmetrical configuration the worst nodal line position is obtained for a  $\rho/\rho_{Ref.}$  value of 1.0, whereas for the symmetrical store carriage the nodal line is already shifted forward for this condition.

Following the experience gained from analyses and model testing, differences in the flutter behaviour of symmetrical and asymmetrical configurations can be affected by

- . reduction of generalized mass for the asymmetrical case which is easier to excite and therefore may lower the flutter speed
- . change of mode shapes on the unloaded wing side, which at frequencies of the three store modes shows contributions of the wing bending mode only. The loaded wing side only exhibits wing torsional motions in the pitch mode, capable to initiate flutter. Energy transfer from the loaded side to the unloaded side therefore results to a more stable overall configuration
- . changed nodal line position of the pitch mode which seems to be the most important effect of unsymmetries because this can shift the minimum flutter speed to a condition, at which the symmetrical configuration may be less critical
- . increased wing bending frequency and decreased store roll frequency for the asymmetrical case which can create a coupling with the store pitch mode by smaller aerodynamic forces than necessary for symmetrical configurations to obtain the flutter condition.

The differences between symmetrical and asymmetrical store flutter seems to be reduced for mild flutter cases if actual values of structural damping as measured in ground resonance tests are considered.

#### Analytical Results for Different Stores Carried on Inboard and Outboard Wing Pylons

The flutter behaviour will now be discussed in detail for different inboard and outboard store conditions.

One of the largest stores usually being carried on the wing is the external fuel tank. For most aircrafts the lowest flutter speed will be obtained for the maximum fuel condition, representing large values of store weight and store radius of gyration which generate flutter according to the "right-hand" flutter branch.

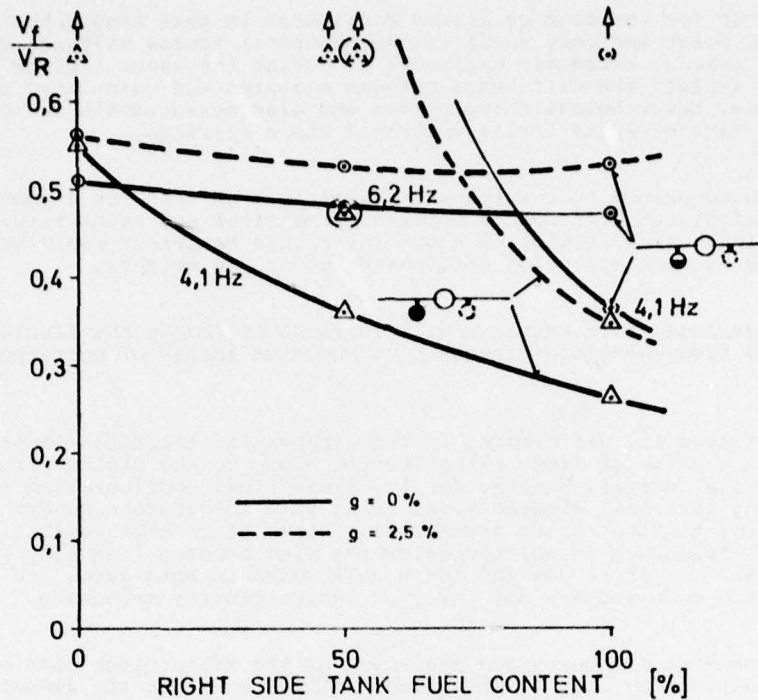


FIG. 5 ASYMMETRICAL FUEL EMPTYING OF INBOARD PYLON TANKS

LEFT HAND TANK: 100% and 50% FUEL  
RIGHT HAND TANK: 0 - 100% FUEL

M = 0.9, WET WING,  $\Lambda = 25^\circ$ , PYLON STIFFNESS 80% OF NOMINAL

Fig. 5 demonstrates the variation of flutter speed with asymmetrical fuel emptying of the inboard pylon tanks at a wing sweep position of 25 degrees. The internal wing tanks are considered to be full because in normal flight operation the external tanks are emptied before the wing fuel is being consumed. For the lower curve one external tank is assumed to contain maximum fuel whereas the fuel of the other tank varies from zero to 100%. The lowest flutter speed is reached for the fuel state with both tanks being full which matches about the minimum flutter speed condition for this configuration. Emptying only one of the tanks, the wing bending frequency lies above the store pitch frequency which provides a very mild flutter at considerably higher flutter speeds.

The upper curve demonstrates the flutter trend of the tanks when the fuel state of one tank is kept in the 50% condition and the other is being varied from zero to 100%. Two different flutter modes are obtained, a very mild flutter at 4.1 Hz when at least one tank is about full and a more excessive flutter at 6.2 Hz which is dominated by the pitch mode of the tank with 50% fuel content. For this configuration it is proved by the results shown in the diagram that all symmetrical and asymmetrical fuel state conditions, which may occur during operational flight or may result from fuel emptying failure cases, are covered by the flutter speed of the symmetrical configuration with full tanks.

How the flutter behaviour changes if outboard stores are added to these tank configurations is illustrated by the next figures.

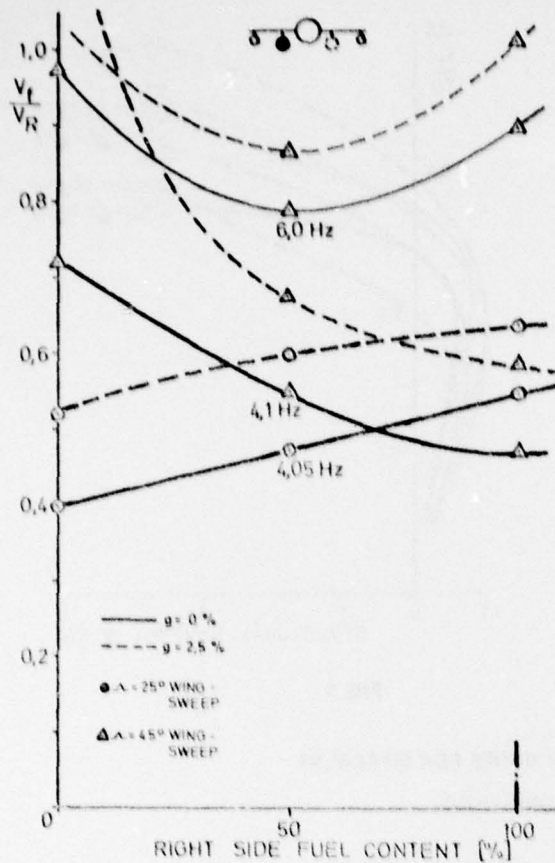


FIG. 6

LEFT HAND TANK 100% FUEL  
RIGHT HAND TANK 0 - 100%

M = 0.9, WET WING, PYLON STIFFNESS 80% OF NOMINAL

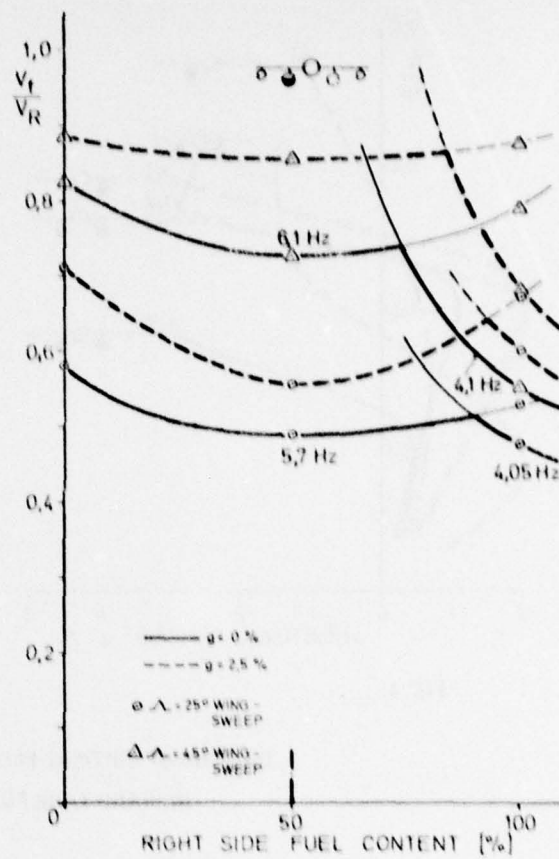


FIG. 7

LEFT HAND TANK 50% FUEL  
RIGHT HAND TANK 0 - 100% FUEL

M = 0.9, WET WING, PYLON STIFFNESS 80% OF NOMINAL

### ASYMMETRICAL FUEL EMPTYING OF INBOARD PYLON TANKS WITH SYMMETRICAL OUTBOARD STORES

In Fig. 6 the results are presented which have been achieved for two different wing sweep positions. One external tank is assumed to be full and the other tank varies from zero to 100 % fuel state. For the 25 degree wing sweep position the highest flutter speed was calculated for the symmetrical full/full condition. Emptying one tank only the flutter speed is decreasing and reaches the lowest value at the empty/full condition. This behaviour is not changed if a relatively large value of 2.5 % structural damping is considered, which proves, that the damping gradient in the flutter point is comparable for symmetrical and asymmetrical fuel conditions. This trend changes to the opposite if the wing is swept back. In this case the symmetrical full/full condition represents the worst condition and would clear also the flutter of asymmetrical fuel states. The second flutter mode at 6.0 Hz is not important for flutter because it indicates higher flutter speeds for all fuel states.

Fig. 7 shows the flutter speeds as resulted for the same store configuration if one tank is being kept in the 50 % fuel condition. For the 25 degree wing sweep position the results are similar to those obtained for the tank configuration without outboard stores (see Fig. 5). Considering 2.5 % structural damping, the lowest flutter speed occurs for the symmetrical condition.

At 45 degree wing sweep the lowest flutter speed is achieved for the 50 %/100 % fuel condition which was already included in the diagram shown before. It is striking that all results obtained for the tank fuel emptying reveal only little effect of asymmetries on the second flutter mode which is dominated by the store pitch mode of the tank with 50 % fuel, coupling with the wing bending mode at a frequency of about 6 Hz. This is also evident from the flutter speed/damping curves for the inboard store carriage shown in Fig. 8.

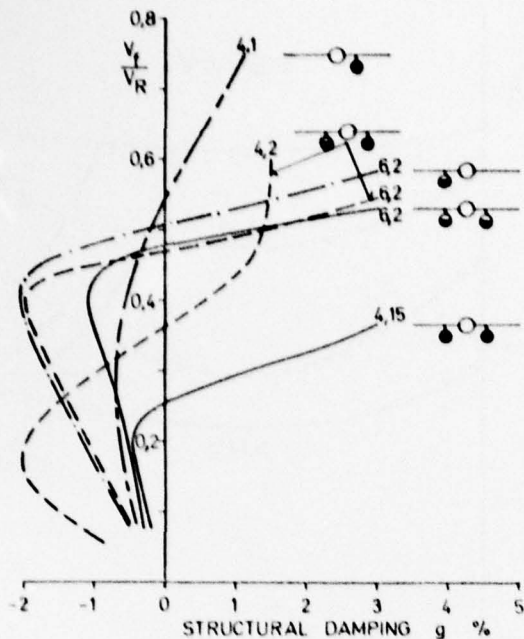


FIG. 8

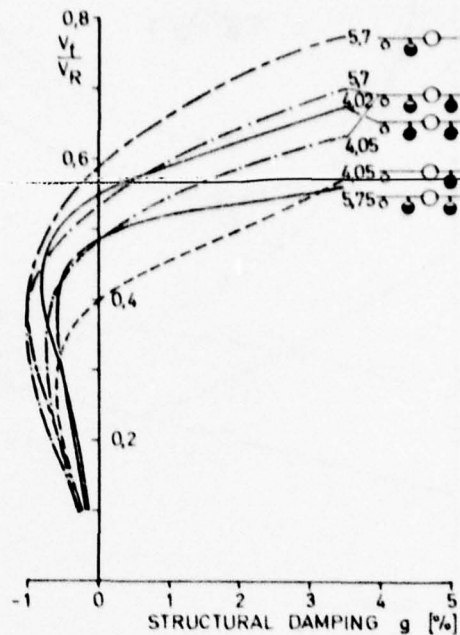


FIG. 9

#### DAMPING OF CRITICAL FLUTTER MODES FOR DIFFERENT INBOARD TANK FUEL CONDITIONS

M = 0.9, WET WING,  $\lambda = 25$ , PYLON STIFFNESS 80% OF NOMINAL

The 6.2 Hz flutter modes are closely spaced for all possible tank combinations whereas the 4.1 Hz flutter modes exhibit a wide scatter of the flutter speed and also of the damping gradient. This phenomenon indicates that the effect of asymmetries on flutter is large if the considered store radius of gyration is close to the value which defines the minimum flutter speed. Figure 8 also demonstrates for this special store configuration that in agreement with common flutter philosophy the flutter speed calculated for the symmetrical configuration would be safe for all possible asymmetrical conditions, not dependent on structural dampings measured for this aircraft in ground resonance test. But deviation from this rule is proved by Fig. 9 which shows the critical flutter modes for the same configurations but carrying in addition stores on the outboard wing stations. In this case the flutter speed resulted for the full/full condition would not be safe for the asymmetrical empty/full tank configuration which flutters at considerably lower air-speed, indicating about the same decrease of damping.

The favourable or unfavourable effect of asymmetry, dependent on the fact whether additional stores are carried on the outboard wing station, can be explained by the decrease of the wing bending frequency due to the outboard store. For the symmetrical full tank configuration this effect is beneficial because it detunes the wing bending and store pitch frequencies whereas for the asymmetrical tank this frequencies are tuned by the reduction of the wing bending frequency. Now also for asymmetrical configurations the wing bending frequency is below the store pitch frequency which creates the capability of severe flutter.

The following example illustrates the asymmetrical flutter of an inboard wing store attached by adapter which reduces the stiffness of the pylon. Due to this reduction in stiffness the considered store radius of gyration for pitch of  $\rho/\rho_{Ref.} = 0.97$  can be expected to match the minimum flutter speed condition for asymmetrical store carriage when the wing is swept to the forward position.



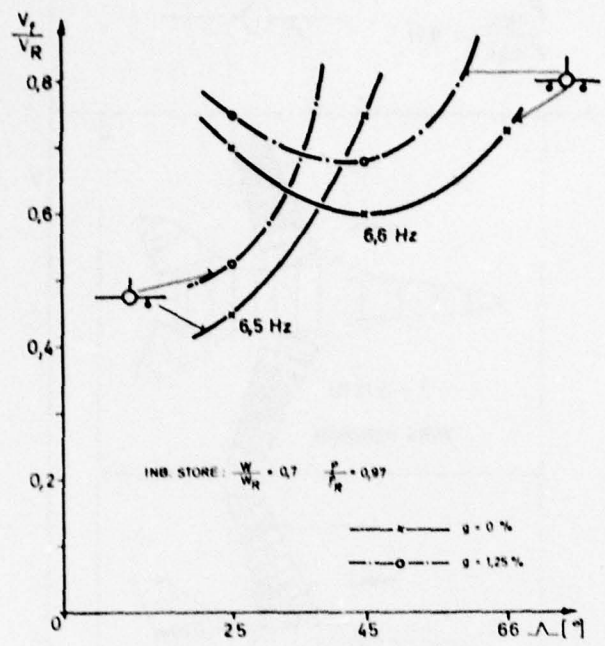


FIG. 10

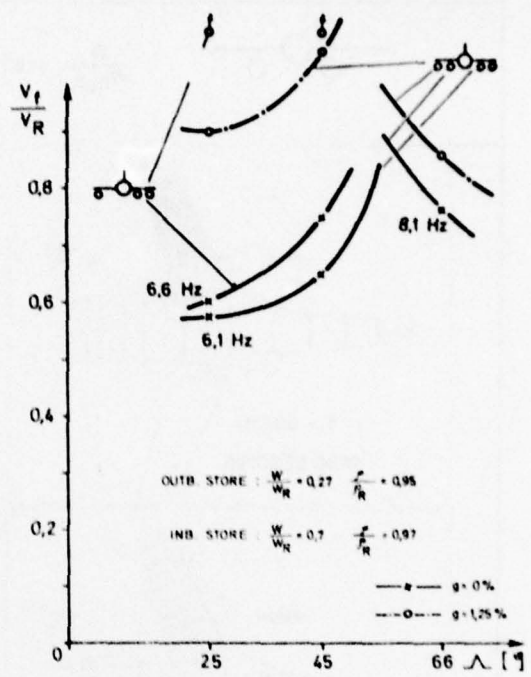


FIG. 11

VARIATION OF FLUTTER SPEED WITH WING SWEEP ANGLE FOR SYMMETRICAL AND ASYMMETRICAL INBOARD STORE CARRIAGE WITH AND WITHOUT SYMMETRICAL OUTBOARD STORES

M = 0.9. DRY WING PYLON STIFFNESS 70% OF NOMINAL

The expected behaviour is confirmed by the results for the inboard store carriage, depicted in Fig. 10 for different wing sweep positions. For 25 degrees wing sweep flutter occurs at considerably lower flutter speed for the asymmetrical configuration. This diagram also demonstrates the large influence of the wing sweep angle on the asymmetrical flutter. At wing sweep positions higher than 35 degrees asymmetrical flutter is not important.

The flutter behaviour is changed completely if additional stores are mounted on outboard wing pylons. Fig. 11 indicates very mild flutter at small and intermediate sweep angles for the symmetrical and also for the asymmetrical store configuration. The critical flutter mode at large wing sweep angles is dominated by the outboard store modes and is therefore not effected by asymmetries of the inboard stores.

The flutter critical situation for the inboard store configuration at 25 degree sweep angle is depicted in Fig. 12. The shapes of the wing bending and store pitch mode, which are important for this flutter case, are about identical for the wing which carries the store. But frequency separation is better for the symmetrical configuration. From the damping and frequency plot of the four flutter modes up to 10 Hz it can be seen that flutter occurs for both configurations by the coupling between wing bending and store pitch. Due to the higher wing bending frequency at zero air speed the coupling point is reached at lower flutter speed for the asymmetrical store. It is also evident, that store yaw (mode No. 2) and store roll (mode No. 4) are not involved in the flutter mechanism.

The next flutter case which will be discussed now is a more complicated example for the "left-hand" flutter branch, characterized by the store pitch/store roll flutter. Fig. 13 shows the four normal modes which could contribute to the store flutter. For both configurations, the symmetrical and also the asymmetrical, the mode shapes are marked by a strong coupling between store yaw, pitch and roll, due to closely spaced frequencies of the store component modes. The second and also the third mode indicate contributions of store pitch, but the second mode show much larger motion of store roll/wing bending, whereas the twist nodal line of the wing exhibits a less critical forward position.

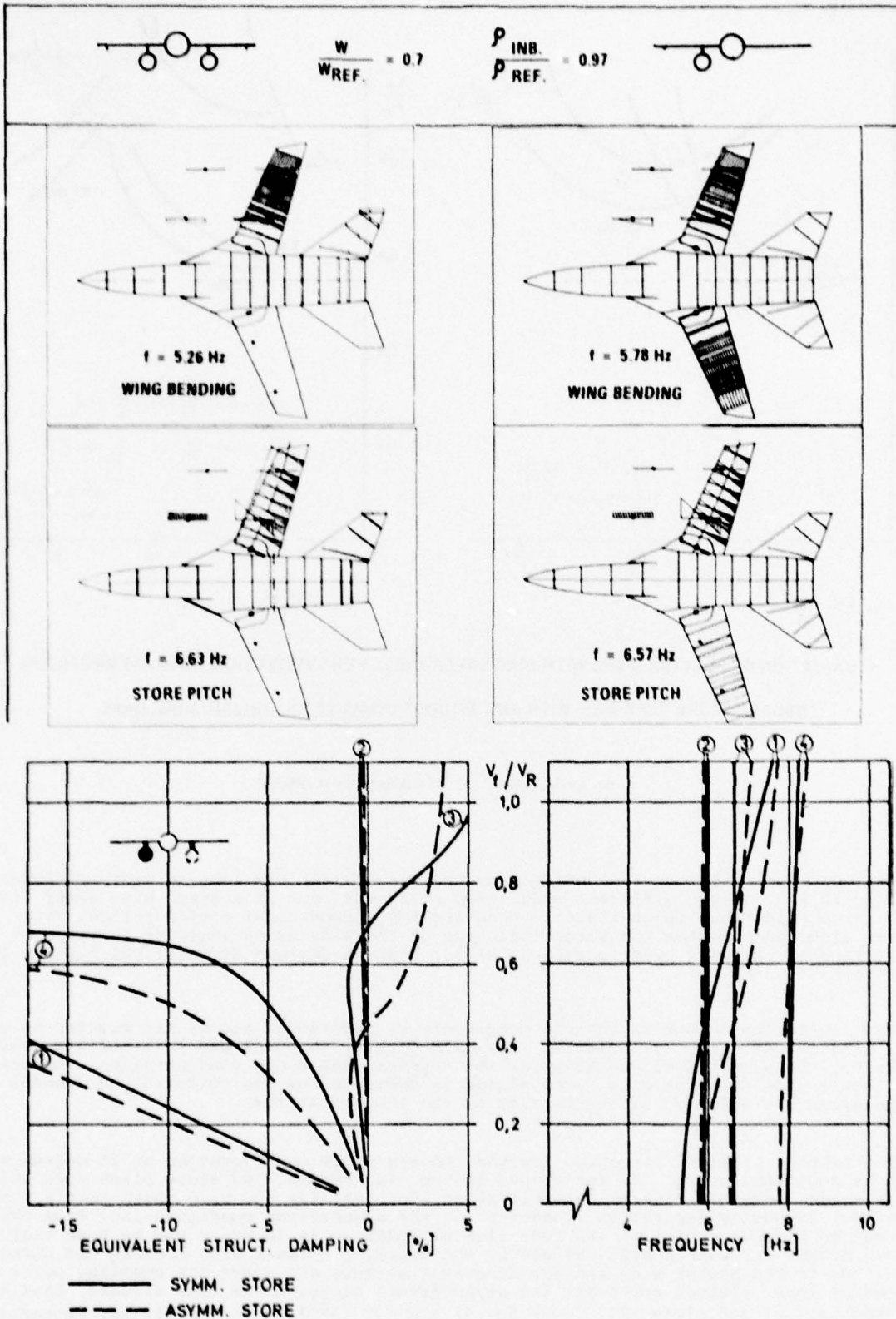
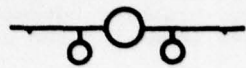


**FIG. 12 SYMMETRICAL AND ASYMMETRICAL CARRIAGE OF INBOARD STORES, ATTACHED BY ADAPTER**

M = 0.9, DRY WING,  $\alpha = 25^\circ$  PYLON STIFFNESS 70% OF NOMINAL



$$\frac{W}{W_{REF.}} = 1.00 \quad \frac{P_{IND.}}{P_{REF.}} = 0.71$$

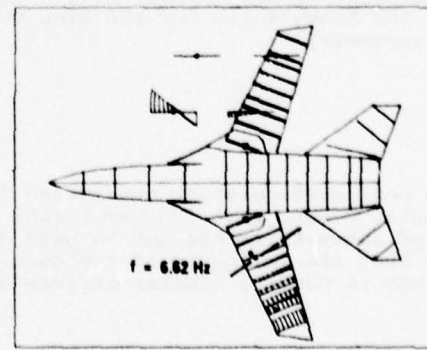
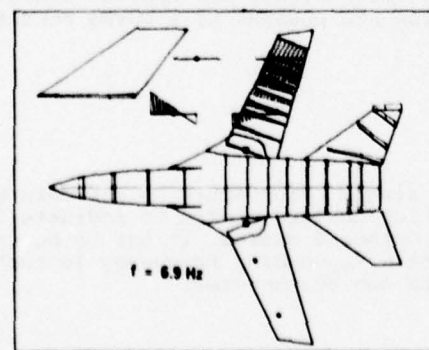
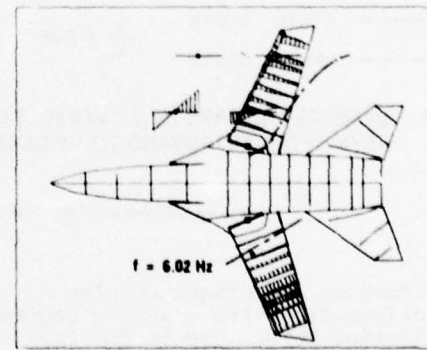
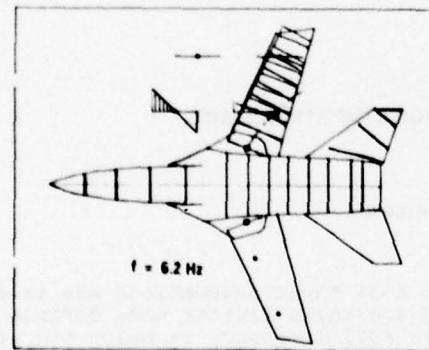
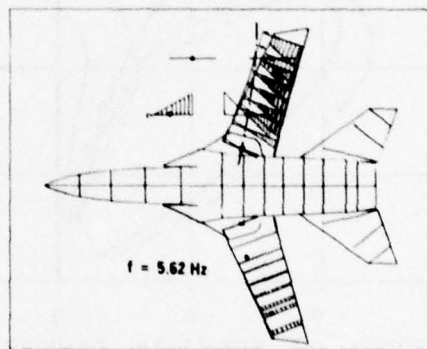
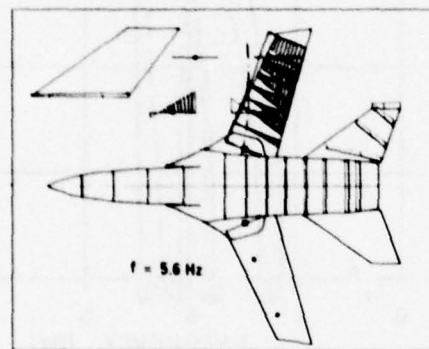
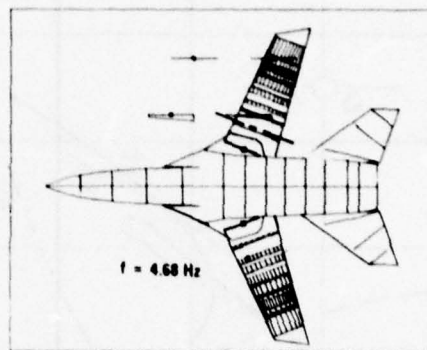
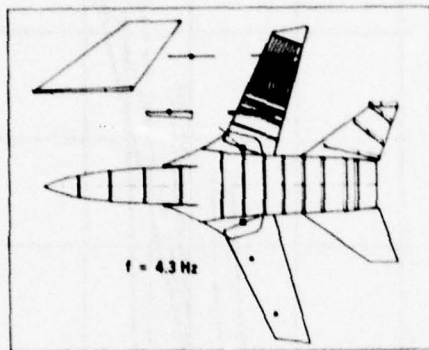
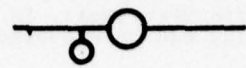


FIG. 13 NORMAL MODE SHAPES OF SYMMETRICAL AND ASYMMETRICAL INBOARD STORE CARRIAGE

It can be assumed, therefore, that the second mode will behave more like a store roll/wing bending mode and the third mode will be the pitch mode which becomes critical. Differences in mode shapes and frequencies between the symmetrical and the asymmetrical configuration are very small. In this case the effect of energy transfer between both sides of the wing can be expected to result to a higher flutter speed for the asymmetrical condition.

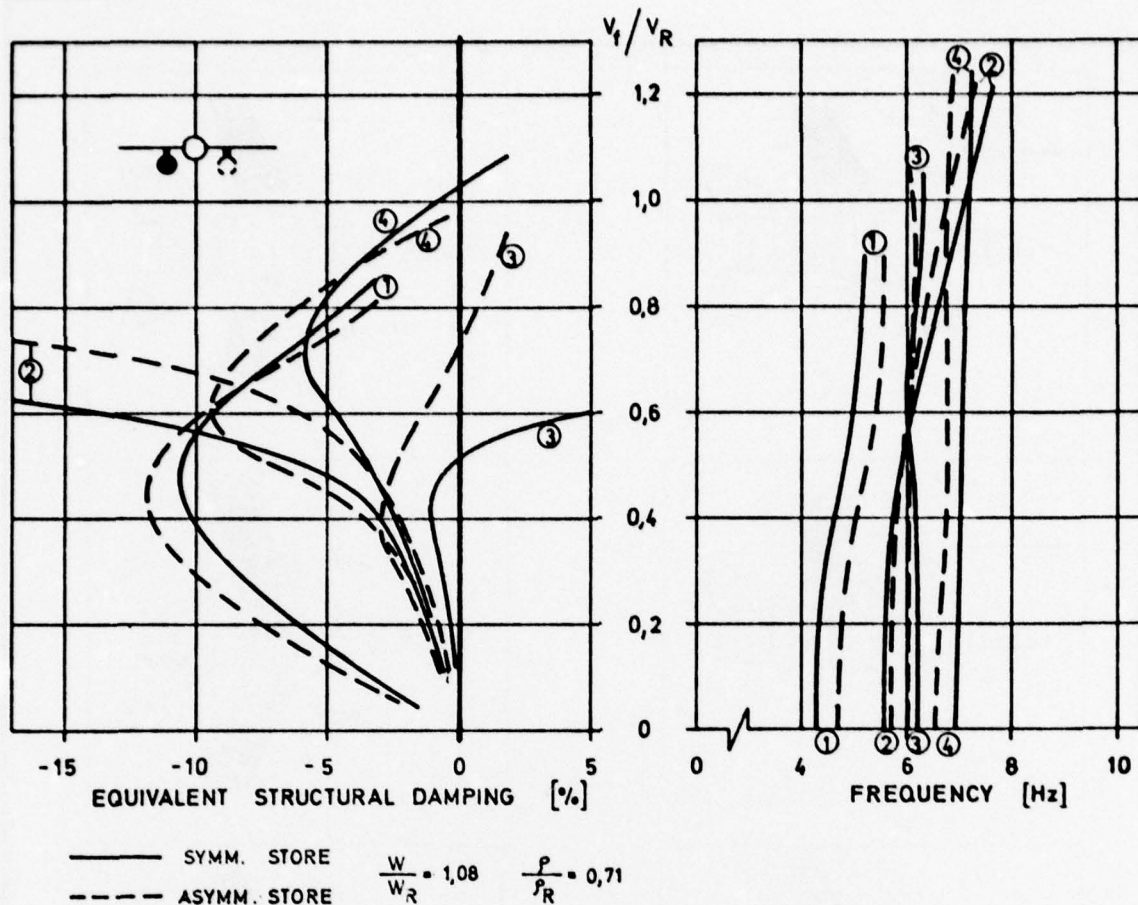
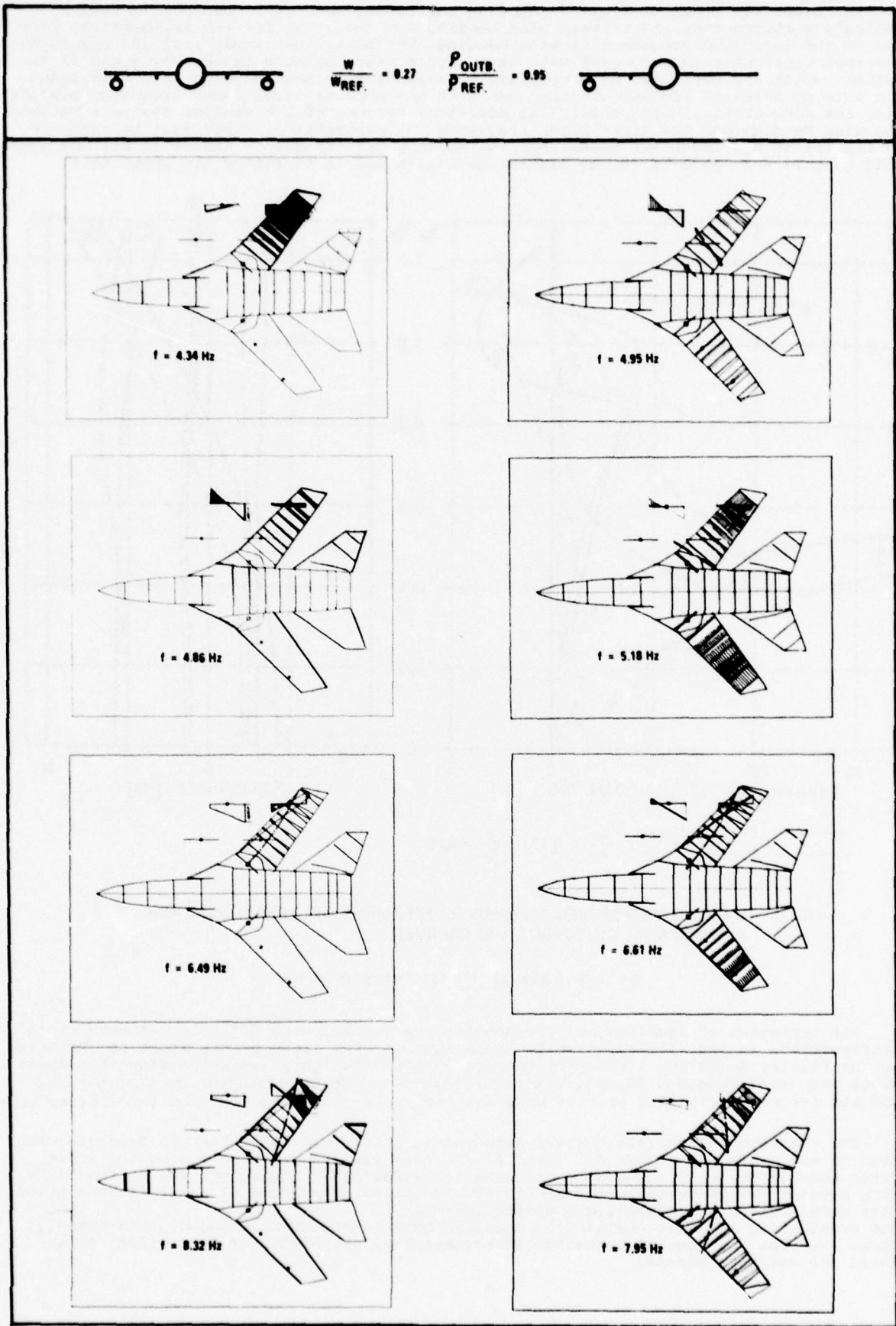


FIG. 14 DAMPING AND FREQUENCY VERSUS FLUTTER SPEED FOR SYMMETRICAL AND ASYMMETRICAL INBOARD STORE CARRIAGE

M = 0.9, WET WING,  $\Lambda = 25^\circ$  PYLON STIFFNESS 80% OF NOMINAL

The damping and frequency plot of Fig. 14 prove that these assumptions are true. For both configurations the coupling between the second and third flutter mode defines the lowest flutter point. Due to the fact that the store roll frequency is below the store pitch frequency, the flutter behaviour of the symmetrical configuration is rather excessive. As expected, the asymmetrical store flutters at much higher air speeds, because neither the frequencies nor the wing twist nodal line are changed to a worse condition by the asymmetry.

The next configuration considered deals with a single pylon store on outboard wing. It is quite clear, that flutter trends established for inboard stores to indicate the effect of asymmetries can not be used directly for outboard stores. It has to be considered that the influence of outboard stores on the wing bending frequency is much larger but in general similar effects of asymmetries can be expected.



**FIG. 15**     **NORMAL MODE SHAPES OF SYMMETRICAL AND ASYMMETRICAL OUTBOARD STORE CARRIAGE**

The first two modes of Fig. 15, showing the normal modes for this configuration, indicate a strong coupling between wing bending and store yaw for the asymmetrical case due to the increased frequency of wing bending. For both, the symmetrical and the asymmetrical configuration, two modes with large store pitch motions (modes No. 3 and 4) are evident which are generated by a coupling between store pitch and wing yaw. Both modes are able to initiate flutter but the mode with the more critical lower frequency exhibits also the more critical wing nodal line position. Because of the smaller distance between the wing bending and the store pitch frequency the asymmetrical store must be expected to flutter at the lower air speed. Due to the very high frequency (about 14 Hz) the store roll mode is not involved in the flutter mechanism and is therefore not shown here.

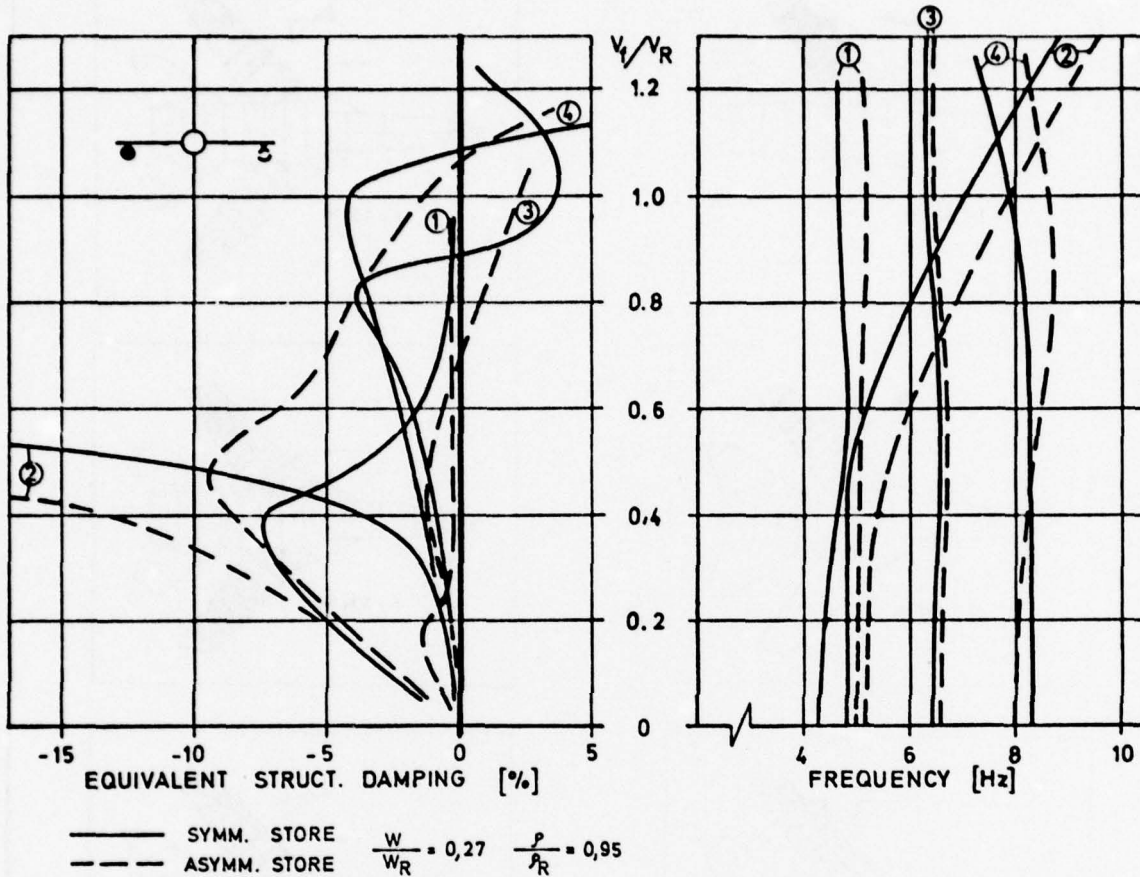


FIG. 16 DAMPING AND FREQUENCY VERSUS FLUTTER SPEED FOR SYMMETRICAL AND ASYMMETRICAL OUTBOARD STORE CARRIAGE

M = 0.9, DRY WING,  $\alpha = 45^\circ$  PYLON STIFFNESS 70% OF NOMINAL

The variation of dampings and frequencies are demonstrated for this outboard store configuration in Fig. 16. The specific behaviour of this light weight store is reflected by the flutter modes No. 1 and 2 of the symmetrical configuration which show that these modes are interchanging. Finally the second flutter mode is dominated by wing bending and the frequency crossing of this mode and the store pitch mode defines the flutter point.

For the asymmetrical store small aerodynamic forces are sufficient to separate wing bending and store yaw (Modes No. 1 and 2). In this case the wing motion of the store pitch mode (Mode No. 3) generates much smaller aerodynamic forces, but due to the higher wing bending frequency the critical flutter condition is reached at lower flutter speed than obtained for the symmetrical configuration. Not considering the more complicated coupling between the modes engaged, this example shows that the fundamental mechanism of asymmetrical store flutter is similar for in-board and outboard stores.

### Effect of Asymmetrical Stiffness Distribution

The last figures presented here demonstrate the effect of asymmetrical pylon stiffnesses on the flutter speed. Two different inboard store conditions are investigated. For the first store a radius of gyration was assumed which matches the minimum flutter speed condition for symmetrical store carriage and which results to higher flutter speeds if only one store is being carried (Fig. 17). For the second store, attached to the pylon by an adapter, a  $\phi$ -value was chosen which is close to the minimum flutter speed condition if the store is carried asymmetrically (Fig. 18). For this case the more critical flutter was found for the asymmetrical configuration with one store only.

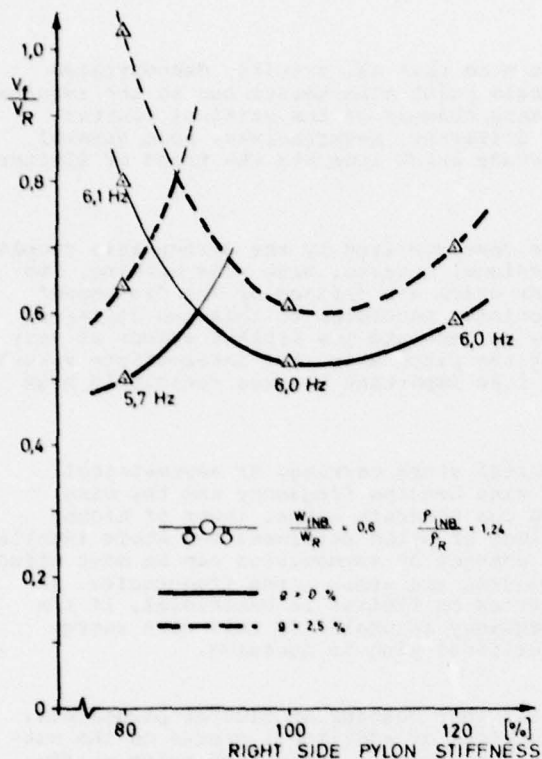


FIG. 17

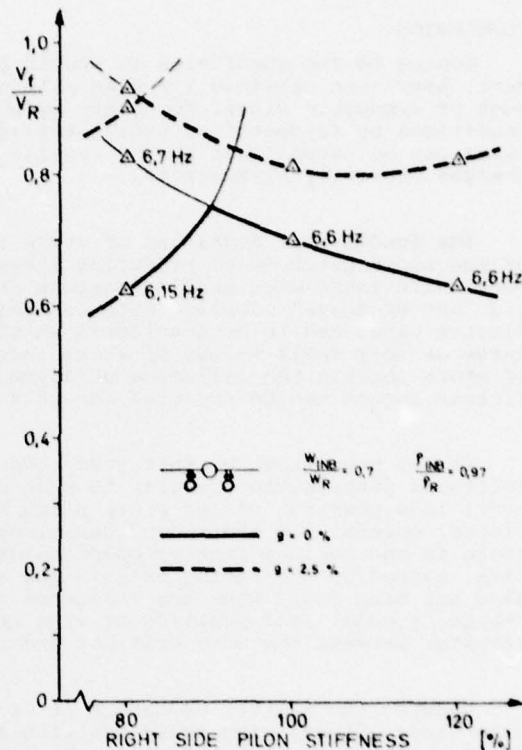


FIG. 18

### VARIATION OF FLUTTER SPEED WITH ASYMMETRY OF INBOARD PYLON STIFFNESS

M = 0.9, DRY WING,  $\Lambda = 25^\circ$ , LEFT HAND PYLON STIFFNESS 100%

In Fig. 17 and 18 the flutter speeds are plotted versus stiffness of one pylon whereas the stiffness of the other pylon is being kept at 100%. Both figures indicate a change of the critical flutter mode when the stiffness of one pylon decreases to 80% of the nominal stiffness.

When the stiffness of one pylon is increased to 120%, a further flutter mode was found at very high flutter speed outside the range of the diagrams. From this the conclusion can be drawn that each wing side creates its corresponding flutter case, each having a minimum flutter speed at defined values of pylon stiffness. For the 6.0 Hz curve in Fig. 17, which refers to the flutter of the pylon with 100% stiffness, the minimum flutter speed is reached at 100% stiffness, corresponding to the  $\phi$ -value which already matches the minimum flutter speed condition at nominal stiffness. For the 6.6 Hz flutter mode of Fig. 18 the minimum is not reached yet, which is reflected by the decreasing flutter speed when the stiffness of one pylon is being increased. Both diagrams also indicate that for the flutter mode related to smaller stiffnesses the flutter speed is still reducing for further reduction of the stiffness.

The results of this calculations demonstrate that asymmetry of pylon stiffness can be very important for values of store inertia and pylon stiffness, which are close to the minimum flutter speed condition. For the cases considered here the influence is reduced, if structural damping is taken into account. For final judgement this phenomenon needs to be further investigated, especially in view of stores having intermediate and smaller radii of gyration. Differences in pylon stiffnesses inside the usual range of small tolerances seems to be less important for flutter but can create considerable problems during the evaluation of flight test data, caused by closely spaced frequencies, which may result to misleading high damping values. In this case a verification of test results by flutter calculations is even more important and it may be necessary to provide the flutter clearance of store configurations with marginal flutter speeds rather by analysis than by flight test.

#### CONCLUSION

Coming to the conclusion it should be kept in mind that all results, demonstrated here, have been obtained for wing pylons with single point attachments, due to the requirement of sweepable wings. For other pylon attachments, changes of the critical flutter conditions by asymmetrical store carriage may be different. Nevertheless, some general rules can be established by the results of this study which indicate the trend of flutter changes caused by asymmetries.

The fundamental mechanism of store flutter is characterized by the aerodynamic coupling of the store pitch mode, producing large wing torsional motions, with wing bending. Two modes with large wing bending motions are existent which are defined by the "in-phase" and "out-of-phase" coupling with lateral store motions. According to this, two different flutter cases had to be considered which are able to generate low flutter speeds at very large or very small values of store inertia about the pitch axis. For intermediate values of store inertia the influence of asymmetries is less important because reasonable high flutter speeds can be expected for this region.

It has been shown by this study that asymmetrical store carriage or asymmetrical stiffness distribution results to changes of the wing bending frequency and the wing nodal line position of the store pitch mode, which can generate either lower or higher flutter speeds. For store configurations with values of pylon stiffness and store inertia close to the minimum flutter speed condition the changes by asymmetries can be most effective, caused by the tuning or detuning of wing bending and store pitch frequencies. It also has been found that the influence of asymmetries on flutter is beneficial, if the change in nodal line position or wing bending frequency is small. In this case energy transfer between the more critical and the less critical wing is decisive.

Knowing the flutter mechanism it is quite clear that changes of flutter parameters, like store weight, wing sweep position and the carriage of additional stores on the outboard wing pylon which influence the wing bending frequency, or changes of pylon stiffnesses which effect the store pitch frequency, will also change the effect of asymmetries considerably as it was shown by the results.

The usual procedure to analyze all store configurations as being carried symmetrically can not be followed for all aircrafts. This does not mean that all possible asymmetrical configurations have to be investigated.

It is recommended to establish flutter trends by variation of important parameters before actual store configurations are being calculated. Once the regions with possibly lower flutter speeds of asymmetrical stores are defined, those configurations can be selected which have to be investigated.

#### ACKNOWLEDGEMENT

The author wishes to acknowledge the help given to him by his colleagues from the flutter department of MBB especially by P. Sichler, who established and ran the computer program for asymmetrical stores and by F. Gresser, who performed the flutter calculations for the symmetrical configurations.



## REFERENCES

- [1] NESS, H.B.  
MURPHY, A.C.  
WILSON, L.E.                      The Experimental Program for Flutter Prevention on the F-111 with Wing Mounted Stores  
  
Fort Worth Division of General Dynamic Corporation, presented at Aircraft/Stores Compatibility Symposium, November 1969
- [2] KATZ, H.                              Flutter of Aircraft with External Stores  
  
McDonnell Aircraft Corporation, presented at Aircraft/Stores Compatibility Symposium, November 1969
- [3] FOUGHNER, J.T.  
BENSINGER, C.T.                      F-16 Flutter Model Studies with External Wing Stores  
  
NASA Langley Research Center, General Dynamics Corporation, presented at Aircraft/Stores Compatibility Symposium, October 1977
- [4] SENSBURG, O.  
LOTZE, A.  
HAIDL, G.                              Wing with Stores Flutter on Variable Sweep Wing Aircraft  
  
AGARD Conference Proceedings No. 162, Specialists Meeting on Wing-With-Stores Flutter, October 1974
- [5] LASCHKA, B.                              Zur Theorie der harmonisch schwingenden tragenden Fläche bei Unterschallanströmung  
  
Zeitschrift für Flugwissenschaften, Vol. 11, 1963
- [6] BECKER, J.                              Instationäre Luftkräfte an Flügel-Außenlast-Systemen  
  
MBB-Report No. UFE-812-71
- [7] BECKER, J.  
SCHMID, H.                              Part II : Unsteady Load Prediction for External Stores  
  
MBB-Report No. UFE-1226, July 1976

## DEMONSTRATION OF AIRCRAFT WING/STORE FLUTTER SUPPRESSION SYSTEMS

Chintsun Hwang\*, Bertil A. Winther\*\*

NORTHROP CORPORATION  
Hawthorne, California 90250

Thomas E. Noll\*\*\*

AIR FORCE FLIGHT DYNAMICS LABORATORY  
Wright-Patterson Air Force Base, Ohio

Moses G. Farmer\*\*\*\*

NASA/LANGLEY RESEARCH CENTER, VIRGINIA

SUMMARY

A wind tunnel test program scheduled for completion in April 1978 is being sponsored by the Air Force Flight Dynamics Laboratory for demonstration of active wing/store flutter suppression systems on a light-weight fighter aircraft. Northrop Corporation was selected as contractor of the program which included preliminary design, final design, fabrication and testing of a wind tunnel model. The present paper presents preliminary results of the design analysis and the test program which was conducted at the NASA/Langley Transonic Dynamics Tunnel. Three configurations were selected for final testing. Two of these configurations were deliberately designed to exhibit low flutter speeds with rapid reductions in damping at the incipient flutter condition. After initial tunnel entries which showed the need for certain improvements in the model and the control system design, substantial increases in the flutter speeds were achieved using both leading and trailing edge control surfaces separately. For the most critical configuration a demonstrated improvement of 18% and a projected improvement of 29% in the dynamic pressure were accomplished.

1. INTRODUCTION

The increase in strength of materials and the use of thin, low-drag airfoils have led to flexible and more flutter-prone wings. With many combinations of external stores, modern fighter aircraft have a wide variety of flutter placards that restrict operational use. In fact, an aircraft carrying external stores may have several flutter speed restrictions on a single flight. In order to reduce the severity of these restrictions and take advantage of recent improvements in controls technology for high-performance aircraft, a logical approach is to develop a flutter suppression system that eventually could employ the same components used for conventional stability augmentation. Before a working flutter suppression system can be installed in an aircraft, a number of design aspects have to be considered. These aspects include selection of control surfaces and related actuation systems, definition of appropriate control laws applicable to a large variety of configurations and flight conditions, and development of redundancy and fail-safe features.

Automatic feedback systems controlling the aeroelastic response have been used successfully on several aircraft. The applications to date have been for augmentation of static stability, improvement of ride quality, reduction of maneuver loads and suppression of structural loads induced by atmospheric turbulence. Considerable interest has emerged in recent years towards adding an active flutter control function to the flight control systems. A pioneering investigation was performed by the Boeing Company and Honeywell, Inc. (1), paving the way for a flight test program that employed an Air Force Flight Research B-52 to demonstrate the feasibility of active flutter suppression. In addition, active flutter suppression tests were conducted on a wind tunnel model of the B-52 to obtain comparisons with flight test data (2). Other efforts within the United States included a wind tunnel test program (3) on an SST-type wing and an analytical study (4,5) of a wing/store flutter suppression system. Outside of the United States, considerable activity in the area of flutter suppression has been evidenced by several publications from England, France and Germany. Significant contributions in terms of wind tunnel test demonstrations include References (6) and (7). An interesting analytical study of active flutter suppression is presented in Reference 8.

In March 1976 the Air Force Flight Dynamics Laboratory (AFFDL) initiated the sponsorship of a wind tunnel test demonstration of active wing/store flutter suppression systems for a lightweight fighter aircraft. Northrop Corporation was awarded the contract which has been accomplished in four phases: preliminary design, final design, fabrication and testing of a wind tunnel model. The present paper presents the design analysis and the test program, which included three entries at the NASA/Langley Transonic Dynamics Tunnel.

2. DESCRIPTION OF THE MODEL

The test specimen is a 30% scale, semi-span (right half) model of a lightweight fighter aircraft. The configuration is characterized by a moderately swept wing with a large, highly swept leading edge extension (LEX) at the root, differential area ruling of the fuselage and under-wing engine inlets with

\*C. Hwang, Manager, Structural Dynamics Research Dept.

\*\*B. A. Winther, Engineering Specialist, Structural Dynamics Research Dept.

\*\*\*T. E. Noll, Aerospace Engineer, AFFDL/FBR

\*\*\*\*M. G. Farmer, Aerospace Engineer, NASA/Langley RC

PRECEDING PAGE BLANK

slots for fuselage boundary layer diversion. The model was designed such that, for three selected store configurations, the unaugmented flutter speeds plus the desired improvements with the AFSS (Active Flutter Suppression Systems) operative, could be demonstrated within the test limits of the NASA/Langley 16-foot Transonic Dynamics Tunnel (TDT). Pertinent scale factors based on freon as the flow medium are presented in Table 1.

The model simulates all important wing, pylon, rigid body, and fuselage degrees of freedom that are required to provide correct modal coupling for flutter. A schematic drawing is shown in figure 1. The wing has an aluminum spar with segmented balsa wood covering. The half fuselage is simulated by a segmented metal shell attached to a magnesium beam which is restrained in its lateral degrees of freedom by three bar mechanisms mounted on the tunnel wall. In addition, the model is supported by a lift cable and by two preloaded (450N) fuselage cables running around pulleys so that the model is free to move in plunge and pitch and, to a lesser degree, in the axial direction. To obtain smooth flow past the fuselage, a splitter plate is installed close to the symmetry plane. The model is trimmed by an all-movable and remotely controlled horizontal tail. A narrow-span leading edge flap and a trailing edge surface were selected as the active flutter suppression devices. They are actuated by miniature hydraulic actuators designed and supplied by the Boeing Company, Wichita Division. Accelerometers are installed inside the wing to sense the vibration. After proper conditioning, the signals are fed to the servo-valve which supplies hydraulic pulses to the actuator. A potentiometer is installed in the hinge mechanism to sense the control surface rotation and provide input to the actuator servo.

DIMENSION	SYMBOL	SCALE
Length	L	0.300
Velocity	L/T	0.451
Time	T	0.665
Frequency	1/T	1.503
Dynamic Pressure	$M/LT^2$	0.127
Mass	M	0.0169
Force	$ML/T^2$	0.0115
Flexibility	$T^2/M$	26.18

Table 1. Model Scale Factors

### 3. ANALYTICAL STUDY

#### 3.1 Initial Flutter Analysis

Several flutter analyses were made to determine the most interesting configurations for the test program. Trend studies were performed with variations of store mass, center of gravity, moment of inertia, pylon attachment, etc. Linearized finite element models of the aeroelastic system were employed in the conventional manner with the dynamic equation formulated in terms of generalized coordinates including a representative number of natural vibration modes and appropriate rigid body modes. Unsteady aerodynamic loadings were computed by use of the doublet-lattice method at three discrete Mach numbers in the subsonic regime. Three external store configurations that differ substantially in the flutter characteristics were selected for further analysis and wind tunnel testing. The configurations are:

Configuration (A): Tip launcher rail: AIM-9E (Sidewinder)  
 Tip pylon (95% span): Not installed  
 Inboard pylon (65% span): AIM-7 Sparrow (3" aft)

Configuration (B): Tip launcher rail: Empty  
 Tip pylon: AIM-7 (3" aft)  
 Inboard pylon: Not installed

Configuration (C): Tip launcher rail: Empty  
 Tip pylon: AIM-9E (6" aft)  
 Inboard pylon: Not installed

Figure 2 presents analytical results for three selected configurations. The preliminary flutter analysis of configuration (A) predicted a "hump" mode at about 13 Hz in model scale with a slow decrease in damping as the flutter speed is approached. As shown in Figure 2, this characteristic results in an unusual increase of the flutter dynamic pressure at Mach numbers approaching unity. Configuration (B) exhibits a conventional bending-torsion type of flutter at around 7 Hz with a violent onset. It should be noted that this flutter condition was created by attaching a wing pylon in the tip region with the store located in an extreme, aft position. Similarly, a violent type of flutter was predicted also for Configuration (C), but (due to the reduced store mass) at the higher frequency 10.5 Hz.

#### 3.2 Design Analysis

Design analyses of the active flutter suppression systems for each configuration were performed to establish control laws, compressibility effects, transducer and control surface locations, etc. For this purpose new analytic techniques were developed at Northrop to cope with the frequency-dependence of the control system terms, which render the conventional eigenvalue solution techniques impractical. One

satisfactory solution method used in the present program is the Characteristic Diagram technique suggested by Landahl<sup>(9)</sup> and developed by Northrop<sup>(10)</sup> into an operational program. The method involves plotting of the characteristic equation in the complex plane at a given speed/altitude combination with the frequency as the parameter. Input frequency is specified by a subroutine that computes an automatic frequency sweep. The sweep rate is reduced as a root is approached, thus defining the characteristic diagram with sufficient accuracy. The damping of the dynamic system is determined directly from the shape of the diagram.

Another analysis technique, also developed at Northrop, is the Transfer Function Synthesis (TFS) technique<sup>(11)</sup> which has proven to be both practical and accurate for most of the present design analyses. The TFS technique is a computerized procedure for obtaining closed-form approximations to aeroelastic transfer functions, including the effects of inertial, elastic and aerodynamic forces. The transfer functions are synthesized from analytical frequency response data as ratios of polynomials in the Laplace variable  $S$ . Figure 3 presents typical computed vertical and angular acceleration responses at 70% wing span due to excitation by the trailing edge control surface. The synthesized approximations of these two curves are very accurate and practically coincide with the computed curves. Further examination of figure 3 reveals that the vertical acceleration response contains substantial contributions from modes adjacent to the flutter mode characterized by the sharp peak at 13 Hz. The same general observation was made for all three configurations. When designing a flutter suppression system it was found important to maximize the relative response in the flutter mode so that the active system at nominal gain values performs without undue excitation of the adjacent modes.

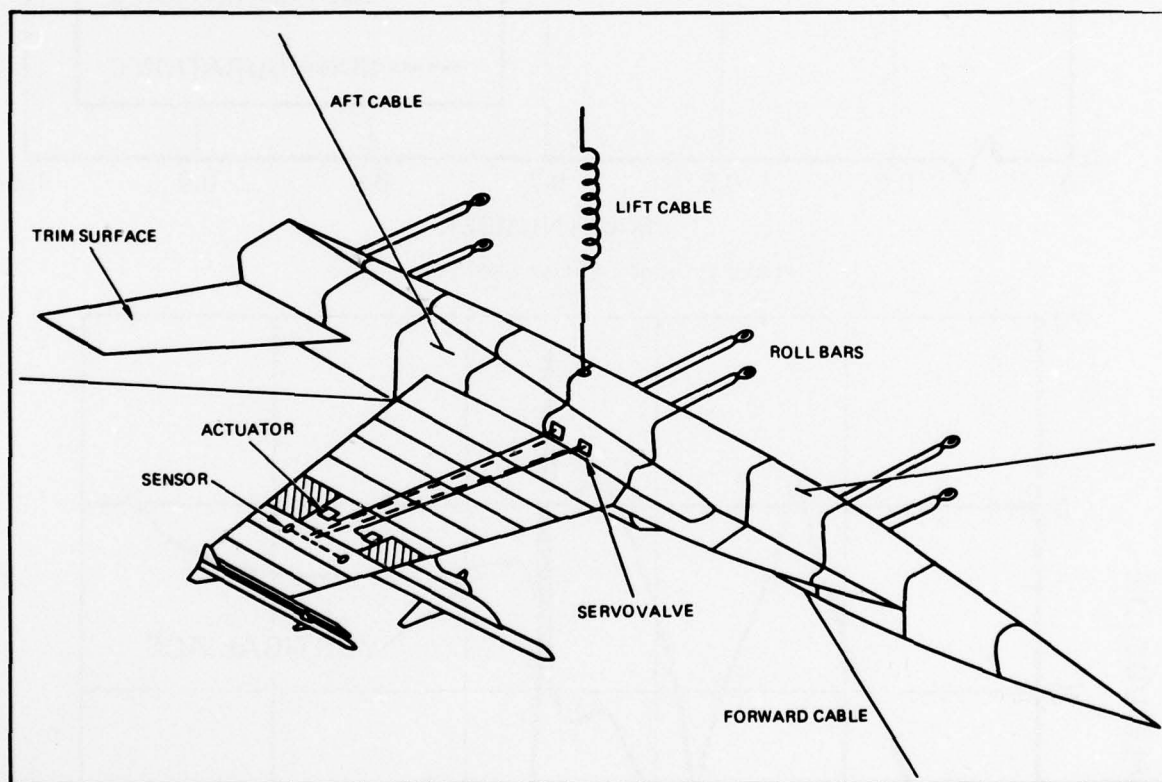


FIGURE 1. WING/STORE MODEL WITH ACTIVE FLUTTER CONTROL CONFIGURATION (A)

The block diagram presented in figure 4 illustrates the flutter suppression system used in the test program. In order to ensure stability of the adjacent modes, several filters are used to condition the feedback signal ( $V_2 - V_1$ ), which is the differential voltage delivered by two accelerometers located at 70% of the wing span. A differential acceleration of one g ( $9.8 \text{ m/s}^2$ ) provides a voltage of approximately 0.2V. Two notch filters at 90 Hz and 34 Hz were required to eliminate ground resonances in the structural panels adjoining the actuator. A second-order low-pass filter (breaking at 42 Hz) was found to eliminate resonance in high-order vibration modes such as the tip missile bending mode. The purpose of the high-pass filter is to minimize the coupling between the structural vibration modes and the rigid-body modes introduced by the suspension system. In the present program, emphasis was placed on simplicity in design and fabrication of the flutter suppression system. To satisfy this requirement it was found that the most desirable filter for compensation of the flutter mode is a first-order variable gain/phase network

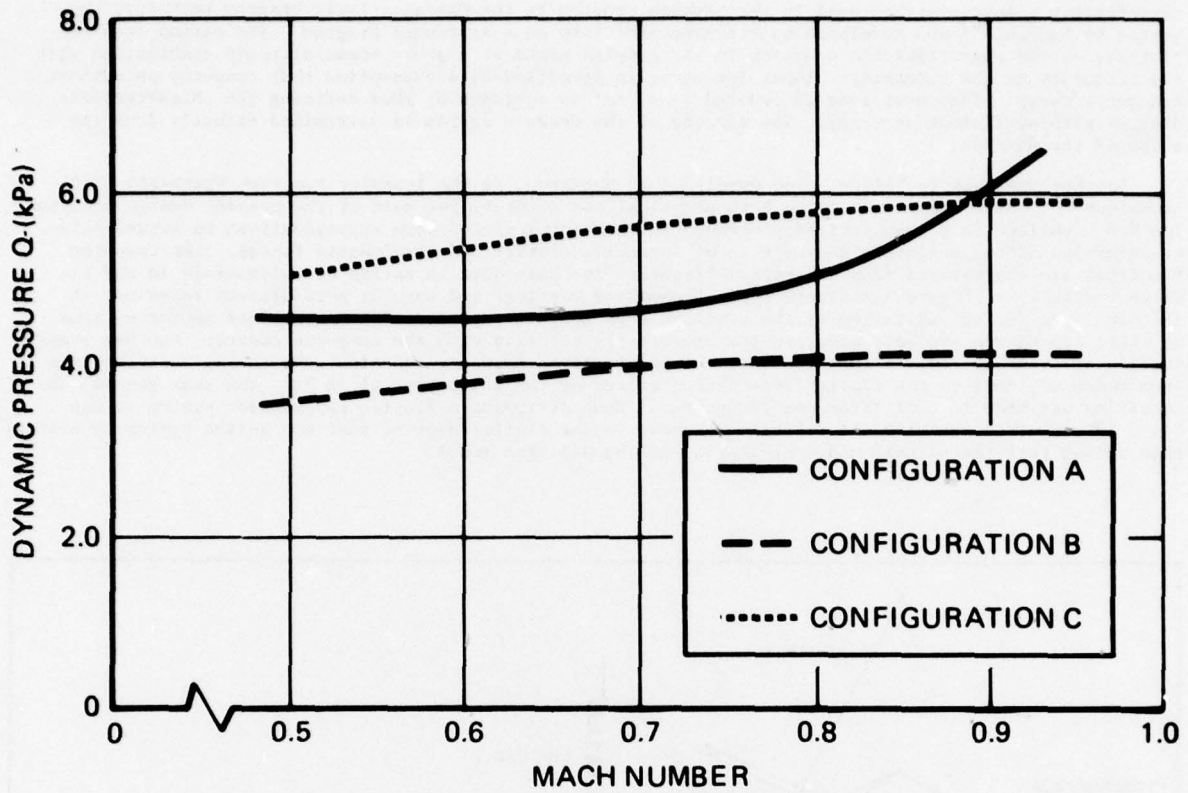


FIGURE 2. MODEL FLUTTER BOUNDARIES

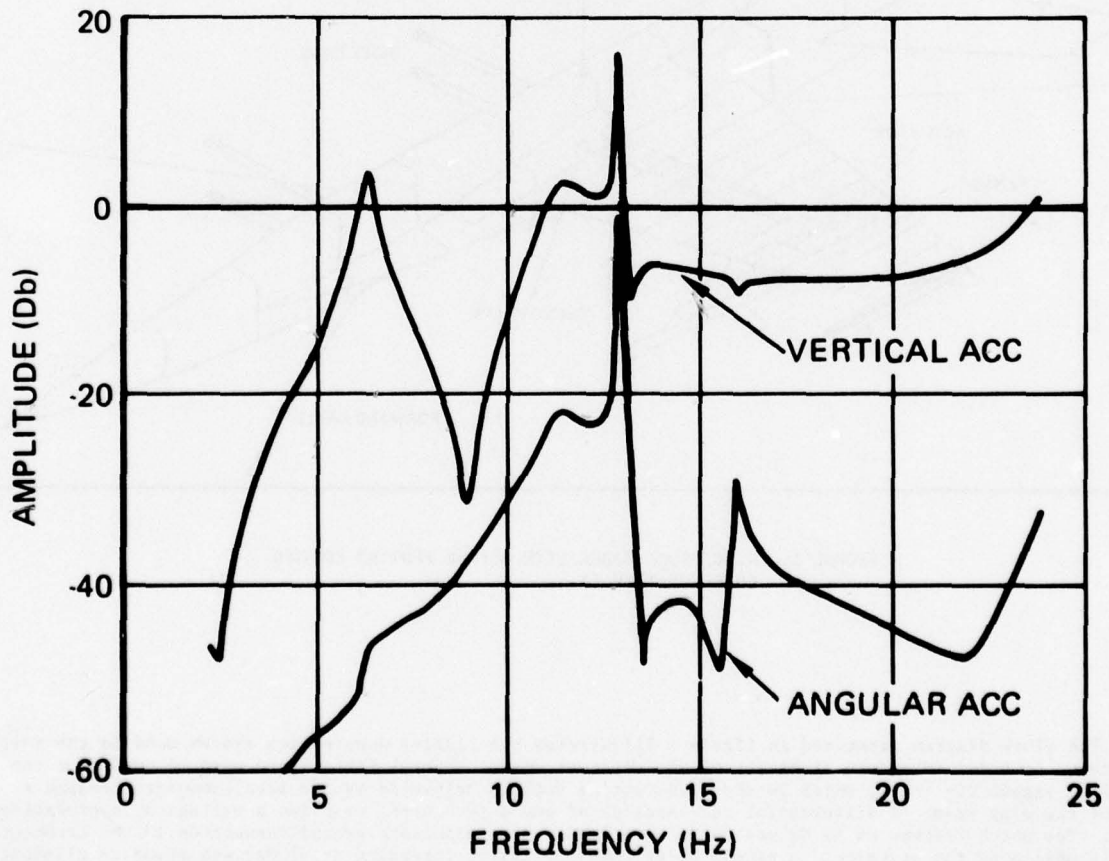


FIGURE 3. VERTICAL AND ANGULAR ACCELERATION DUE TO TRAILING EDGE CONTROL INPUT, 200 KTAS, CONFIGURATION (A)

as shown in the block diagram. A dial on the control panel is used to adjust the gain values in the range 0.0-2.0. Similarly, using another dial, the time constant  $\tau$  of the phase compensation can assume values between 0.0 and 0.05 seconds.

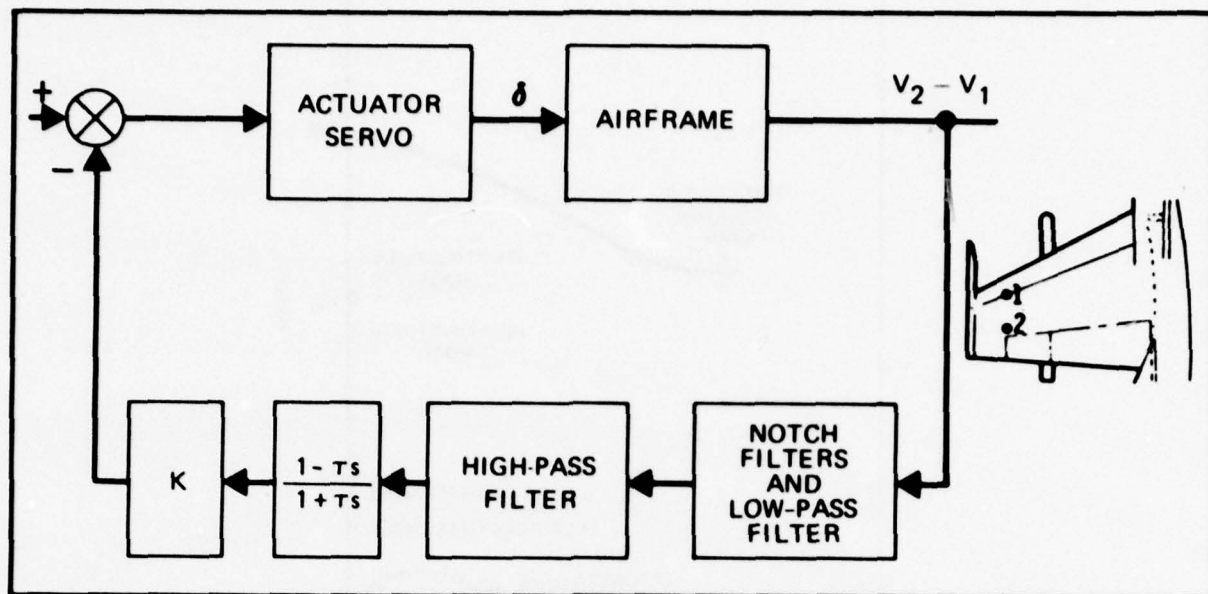


FIGURE 4. BLOCK DIAGRAM OF THE FLUTTER SUPPRESSION LOOP

Extensive analyses were performed to determine the optimal gain-phase settings for various dynamic pressures and Mach numbers. The approximations of the aeroelastic response at various speeds and Mach numbers were used to obtain root locus plots with the loop gain as parameter. Figure 5 presents a typical root locus plot for configuration (B) with leading edge control, at a speed slightly exceeding the flutter speed. It is observed that all poles associated with structural vibration modes are located close to the imaginary axis. Another finding is that the flutter suppression system has an adverse effect on the first wing bending mode which becomes unstable at high loop gains. Due to this limiting factor on the allowable loop gain, the flutter suppression system is able to stabilize the system only up to moderate dynamic pressures as demonstrated in Figures 6 and 7 which present magnified views of the roots associated with the first two structural modes. All roots associated with the actuator servo and the filters are sufficiently stable for normal gain values.

Similar analyses were performed for the other configurations with both leading and trailing edge controls at various Mach numbers. The trailing edge system for configuration (A) was found to be very effective in suppressing the "hump" mode flutter. For configuration (C), as for (B), the analysis predicted that the leading edge surface would be more effective in controlling the flutter mode. For both configurations, however, the allowable gain was limited by the destabilizing effect predicted for the root associated with fundamental wing bending.

#### 4. GROUND VIBRATION TEST

The initial ground vibration test (GVT) was conducted at Wright-Patterson Air Force Base in Ohio during April 1977. Two different types of vibration tests were performed. The conventional type utilized discrete, sinusoidal shaker input at each natural frequency. Relative accelerations were measured by a roving accelerometer. Due to the time-consuming nature of this test, it was completed for configuration (A) only. The second type of GVT utilized a Hewlett-Packard Fourier Analyzer, System 5451B operated by the Dynamics Test Group at AFFDL. The wind tunnel model was excited by random noise input to a shaker located in the fuselage nose. The response was measured consecutively at preselected stations and transmitted to the computer. Almost simultaneously with the data transmittal, the transfer function for each test point was computed and stored on disc. Sampling time per point was approximately 120 seconds and the resulting frequency resolution was 0.2 Hz. The transfer function data stored on disc were used to determine the modal deflections at approximately 85 points for each of the three configurations. To extract accurate measurements of the modal damping, a zoom technique was employed with data sampled at a few locations during approximately 600 seconds. Figure 8 presents a typical transfer function computed by the Fourier Analyzer. Even though all modes generated by the Fourier Analyzer between 0 and 50 Hz are clearly identifiable, the shapes of the low-frequency modes show poor correlation with the corresponding modes measured in the conventional GVT or the ones obtained from analysis. The results for higher-order modes are satisfactory. Later, during each wind tunnel entry, the conventional vibration test was repeated to verify the structural integrity of the model and determine the influence of the suspension system.

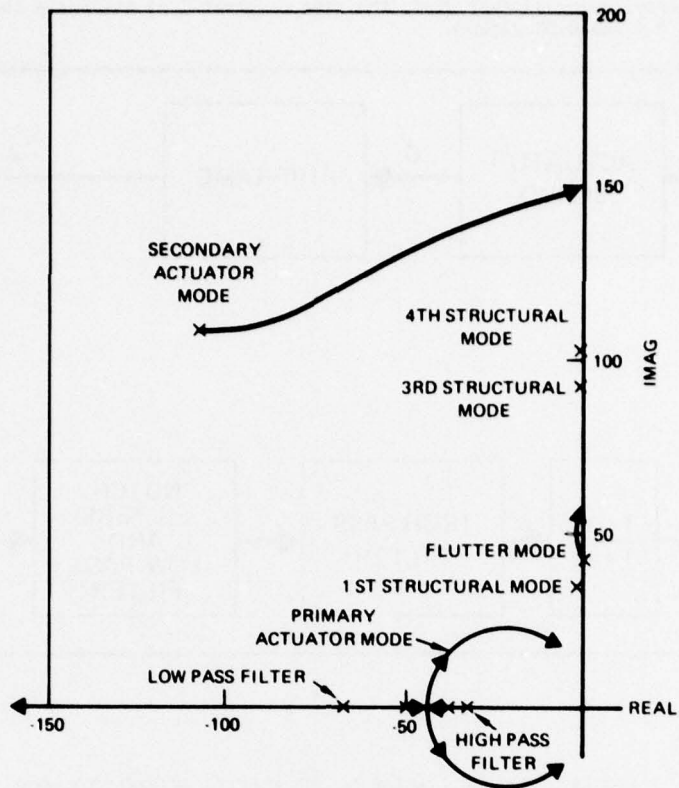


FIGURE 5. ROOT LOCUS OF CONFIGURATION (B) LEADING EDGE CONTROL  $M = 0.0$   
 $V = 370.4 \text{ km/h}$

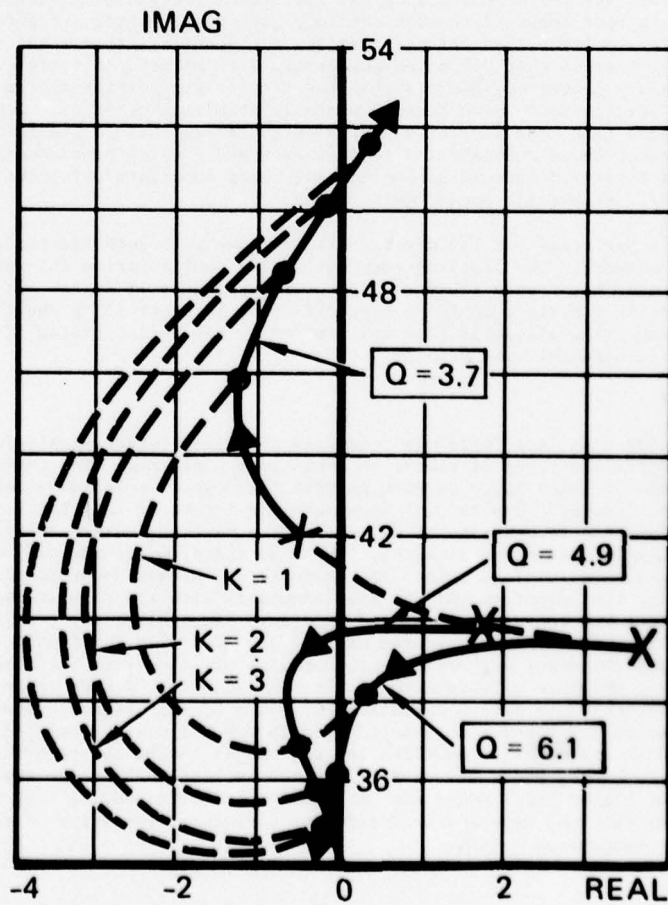


FIGURE 6. FLUTTER MODE ROOT LOCUS, CONFIGURATION (B),  
 LEADING EDGE CONTROL  $M = 0.8$

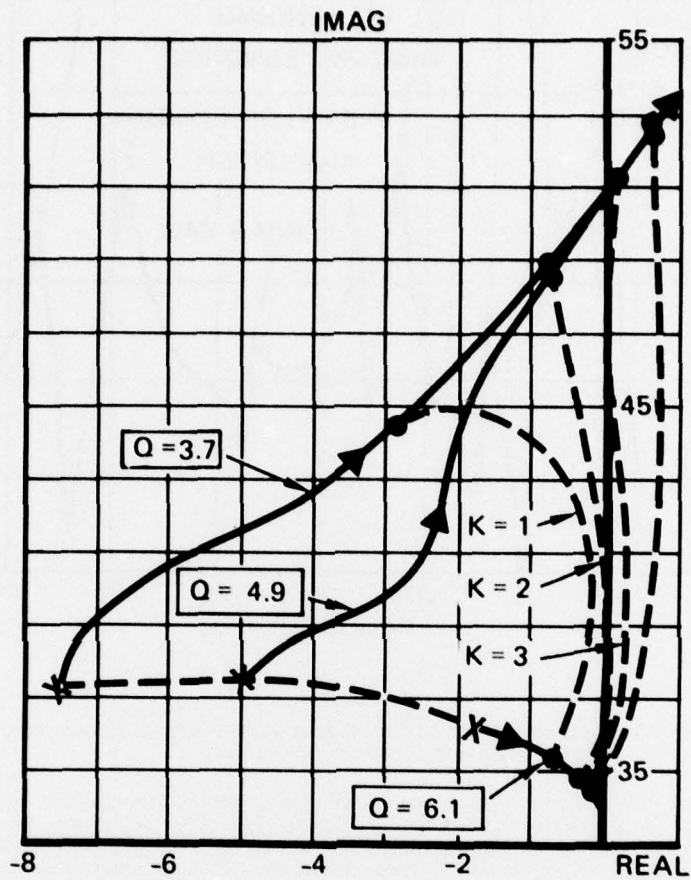


FIGURE 7. FIRST BENDING MODE ROOT LOCUS, CONFIGURATION (B),  
LEADING EDGE CONTROL  $M = 0.8$



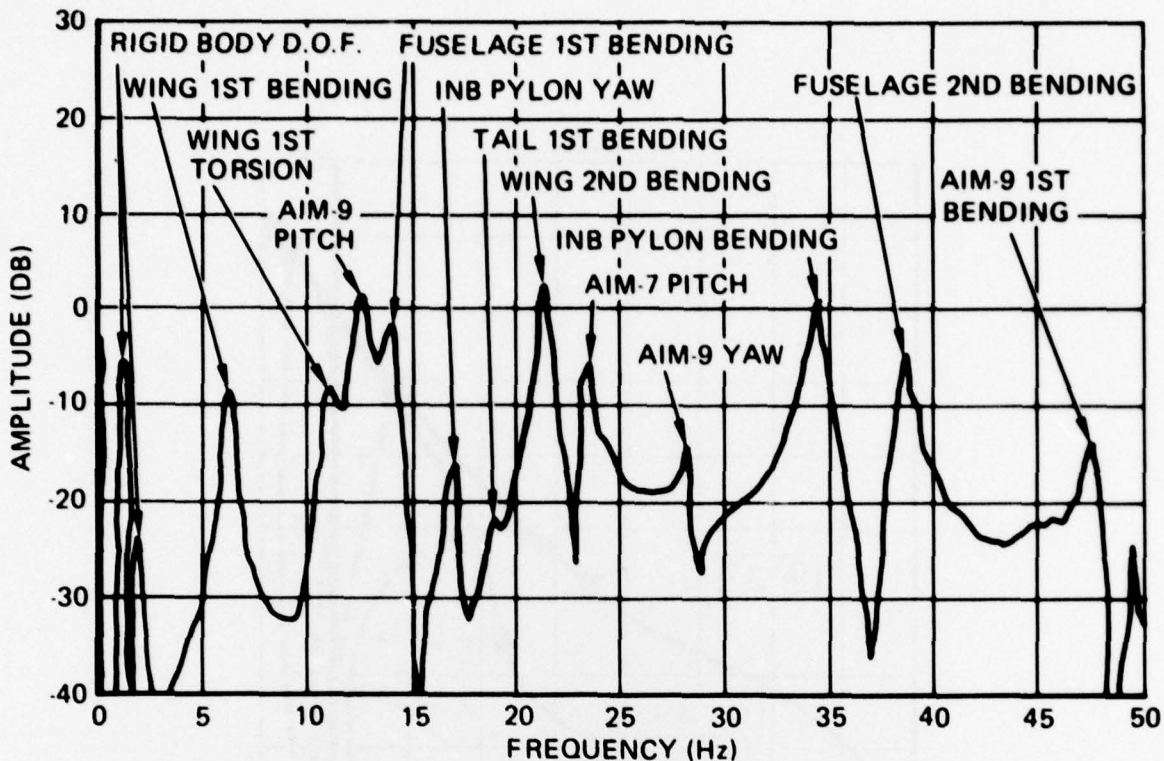


FIGURE 8. ACCELERATION AT LEADING EDGE PICKUP DUE TO RANDOM INPUT AT FUSELAGE NOSE, CONFIGURATION (A)

Functional checks of the actuator servos and other components in the control system were made both in a bench test and with the system installed in the model. Open-loop tests were performed to measure the servo output versus input command. The gains of the actuation loop were set for optimum closed-loop response, which then was modified by various filters to match a typical aileron actuator. After completion of the functional tests, the flutter suppression loop was closed to determine the loop gain at ground resonance. Due to the potential danger to the model, precautions were taken to limit the hydraulic flow rate provided by the servo-valve. Notch filters were inserted in the flutter suppression loop to eliminate critical modes. To further increase the available loop gain, the notch filters were modified and a second-order low-pass filter inserted during the second wind tunnel entry.

In addition, a frequency response test was performed. The objective was to measure acceleration responses due to control surface inputs and store the data on magnetic tape for future processing. From the input and output signals of the actuator servo, a transfer function as shown in figure 9 was derived and compared to the discrete data measured in the functional test. The low-frequency response of the actuator servo is referenced to 3.8 degrees/volt. After the first wind tunnel entry, the servo was completely redesigned and the frequency response was modified to some extent in the high-frequency band.

## 5. WIND TUNNEL TESTS

### 5.1 First Entry

The wind tunnel test program was conducted at the NASA/Langley Research Center in three separate entries during June, August and December 1977. In the first entry, the leading edge surface was used for sweep-excitation of configuration (A). A rapidly diverging oscillation of the leading edge servo was encountered well below the predicted flutter speed.

In reviewing the test results from the first entry, Northrop decided to redesign the actuator servos. A detailed analysis<sup>†</sup> of the leading edge servo was performed considering the destabilizing effect of the airloads. Figure 10 demonstrates that the root associated with an integrator in the forward servo-loop couples with the root associated with the airload on the leading edge control. With maximum attainable loop gain, the analysis shows that the system was only marginally stable. Based on this analysis, the first step was to eliminate the integrator and redesign the servo. At the same time, a number of

<sup>†</sup>The authors acknowledge George R. Mills of Northrop Corporation for his substantial contributions to this analysis.

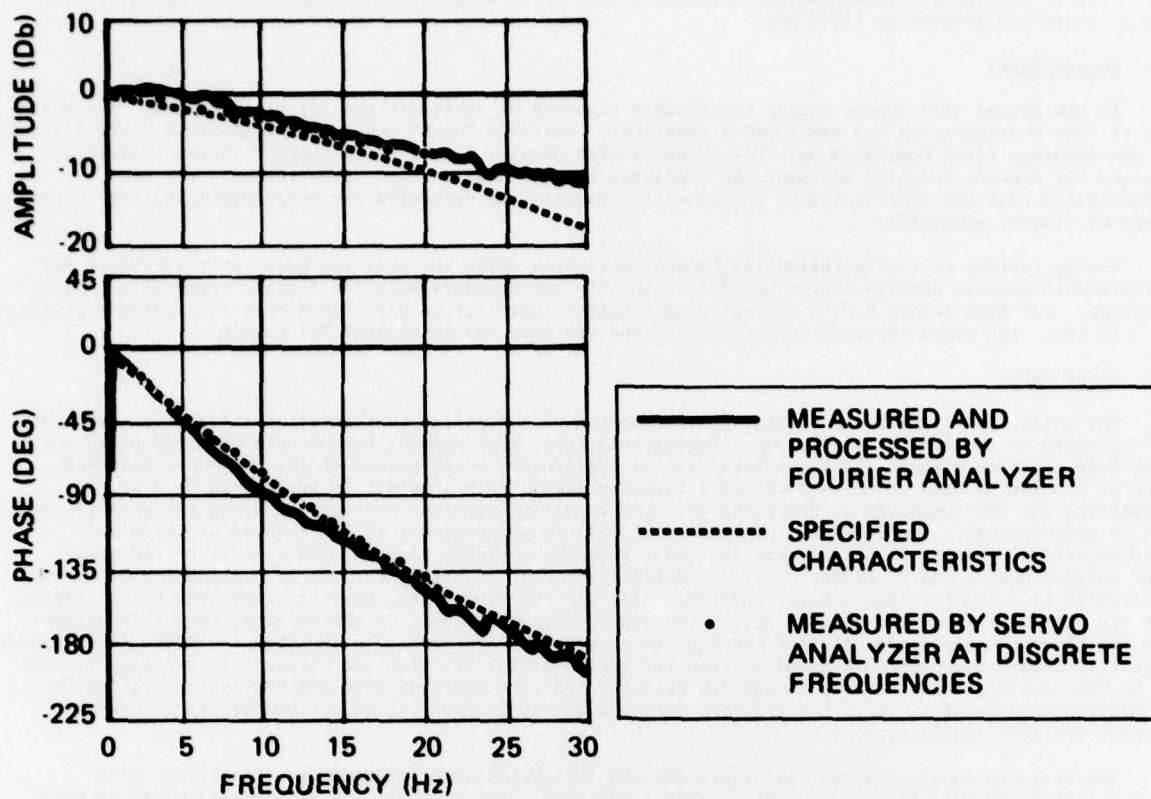


FIGURE 9. TRANSFER FUNCTION OF TRAILING EDGE SERVO

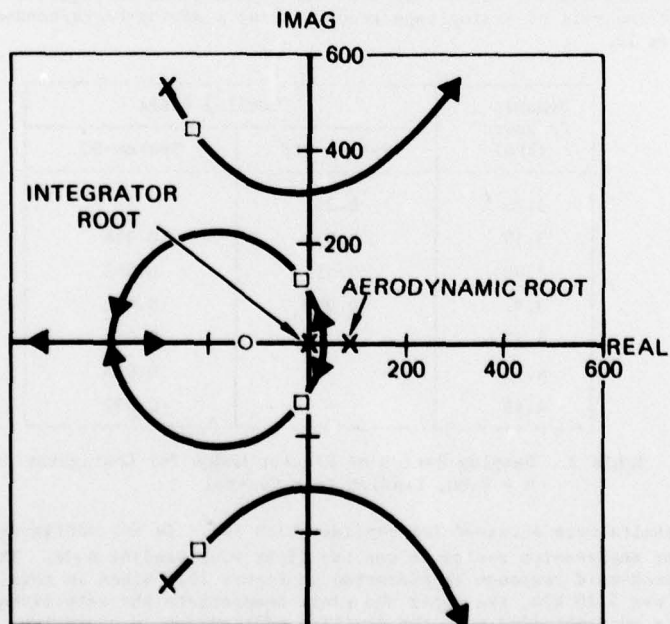


FIGURE 10. ROOT LOCUS OF LEADING EDGE SERVO IN FIRST TUNNEL ENTRY

precautionary measures was undertaken to increase the dynamic stiffness of the servos. The pressure feedback used in combination with position feedback in the servo loop was eliminated and the hydraulic supply pressure was doubled to 13800 kPa.

### 5.2 Second Entry

In the second wind tunnel entry, the flutter boundary of configuration (A) was explored. The analysis of this configuration had predicted a moderately unstable "hump" mode with significant participation of the fuselage first bending mode. Unexpectedly high damping in the model support system, however, changed the dynamic coupling and made the predicted flutter mode stable. Nevertheless, the test demonstrated that the control system increased the damping and decoupled the modes participating in the expected flutter mechanism.

During testing of configuration (B), sweep excitation using the trailing edge control surface was performed to measure damping levels and define the flutter boundary with the flutter suppression system inactive. For Mach number 0.8, a violent wing torsional oscillation was encountered at a dynamic pressure of 3.64 kPa. The model experienced some damage and the test was terminated for repair.

### 5.3 Third Entry

The third tunnel entry was initiated with testing of a modified configuration (A) having a mass of 0.2 kg added to the AIM-9E missile tip. During this test, most damping trends were obtained using the peak-hold spectrum method, which provides Fourier-transformed measurements of the response, filtered through 250 narrow-band circuits. The peak response within each interval is registered on a screen, permitting the test engineer to determine when the resulting spectrum has converged and the data sampling can be discontinued. The damping of a resonating mode is proportional to the inverse of the peak-hold amplitude. Figure 11 illustrates the model response in terms of peak-hold spectra of the wing root torsion moment due to either tunnel turbulence alone or tunnel turbulence in combination with sweep excitation by a leading edge control surface. Although the flutter suppression system was not activated for the test points covered in this graph, the data gives an estimate of the relative tunnel turbulence and the threshold amplitude at which the flutter suppression system can be expected to affect the response. Figure 12 presents a peak-hold damping trend for configuration (A) with and without flutter suppression. As in the previous tunnel entry, it was demonstrated that the trailing edge control system provided a significant amount of damping, but friction in the model suspension system was sufficient to prevent flutter for this configuration.

The test continued with configurations (B) and (C), which were designed specifically to have severe flutter on-set. Figures 13 and 14 present measured damping trends for configuration (B) at Mach numbers 0.6 and 0.8, respectively. The model sustained slight damage at  $M = 0.8$  where a "hard" flutter point was obtained. Subsequently, considerable increases in the flutter speeds were achieved using the leading edge control surface. For configuration (B) at Mach number 0.6, a demonstrated improvement of 18% and a projected improvement of 29% in the dynamic pressure were accomplished. As predicted by analysis, the increased damping in the flutter mode was traded for a destabilizing effect on the first wing bending mode. For this reason, the nominal loop gain in the flutter suppression system was limited to 0.7. The frequency shifts predicted by the analysis for system-on, were also substantiated by the test showing a sudden drop in the torsion frequency as the dynamic pressure approached its critical value. Table 2 presents estimated damping ratios for the data points shown in Figure 14. These results were obtained by post-test analysis of analog tape records using a moving-block/randomdec technique as described in reference 12.

Dynamic Pressure (kPa)	Damping Ratio	
	System-Off	System-On
3.35	0.051	-
3.59	0.030	0.084
3.83	0.014	0.082
3.97	0.000	0.071
4.12	-	0.053
4.31	-	0.045
4.45	-	0.031

Table 2. Damping Ratios of Flutter Modes for Configuration (B)  
 $M = 0.80$ , Leading Edge Control

Similar test results were obtained for configuration (C). As for configuration (B), the critical mode with the flutter suppression system on was the first wing bending mode. The effect of the leading edge system on the peak-hold response is presented in Figure 15. Since in this case the projected dynamic pressure at flutter was 5.10 kPa, the upper two plots demonstrate the effectiveness of the closed-loop system. Similar data were obtained with the trailing edge system in operation. Damping trends at Mach 0.6 are presented in Figures 16 and 17 with the leading and trailing edge systems on and off.

Future flutter suppression systems most likely would be tied to special purpose computers responding in an adaptive manner to counteract the structural response. An alternative and technically simpler approach would be to depend on the flight data computer to provide pre-programmed control laws for various configurations and flight conditions. In the present program, it was observed from both test data and analytical

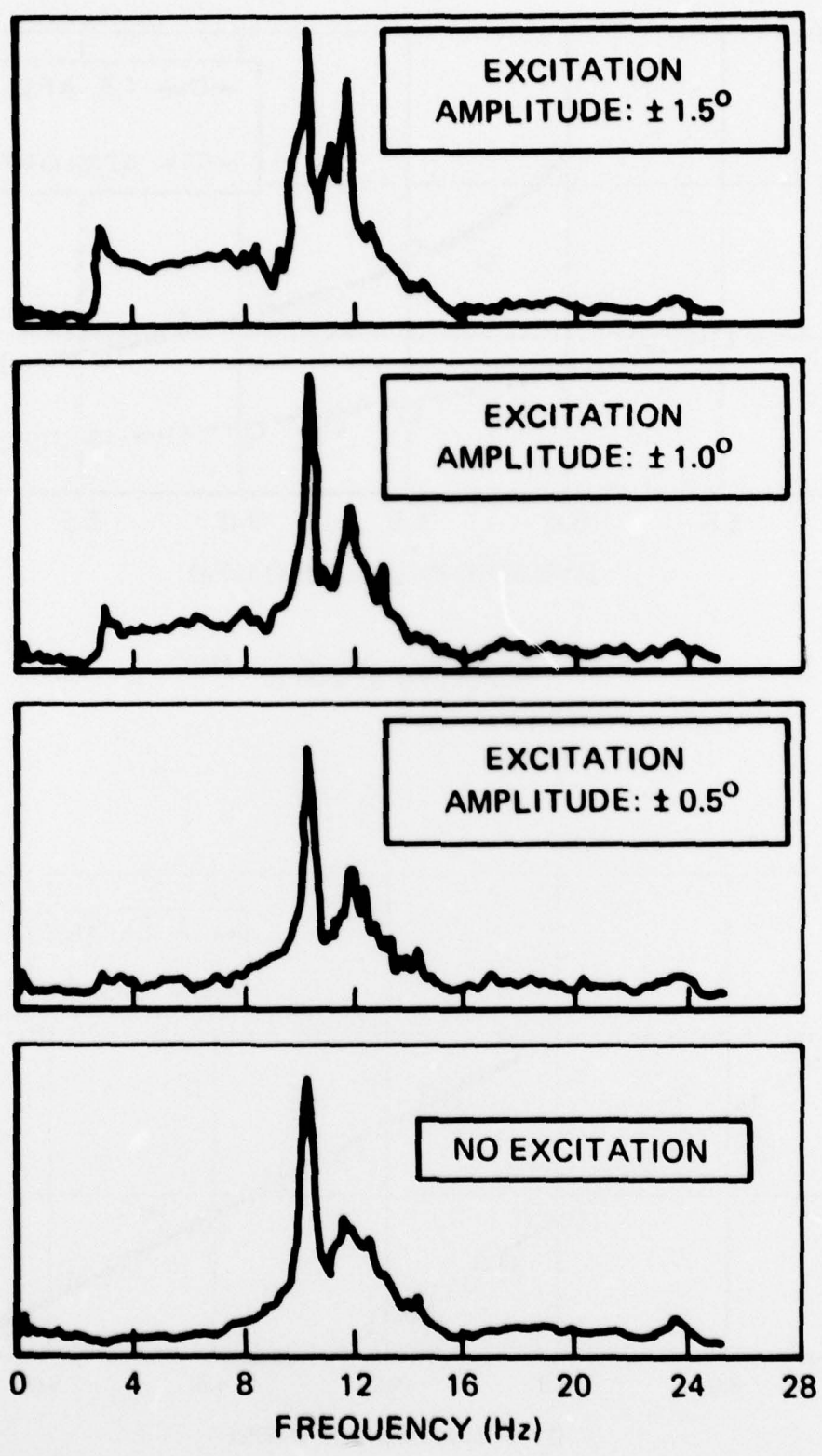


FIGURE 11. PEAK-HOLD SPECTRA OF WING ROOT TORSION MOMENT DUE TO LEADING EDGE CONTROL SWEEP AND TURBULENCE, CONFIGURATION (A)  
M = 0.90 Q = 5.75 kPa

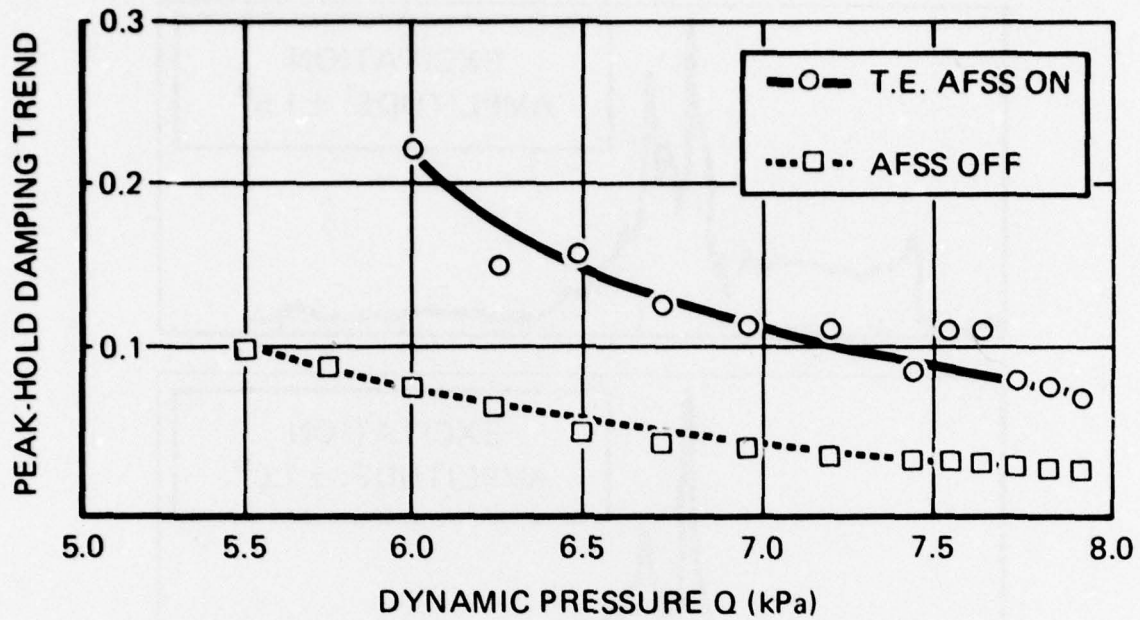


FIGURE 12. DAMPING TREND, TRAILING EDGE SYSTEM CONFIGURATION (A)  $M = 0.80$

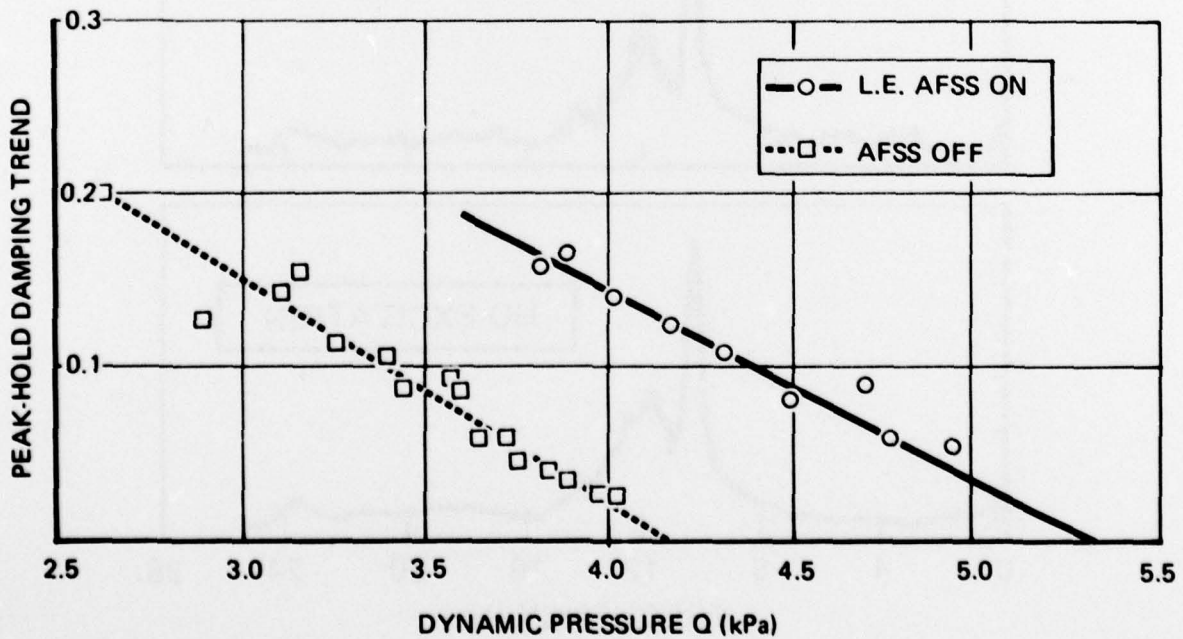


FIGURE 13. DAMPING TREND FOR CONFIGURATION (B), LEADING EDGE SYSTEM  $M = 0.60$

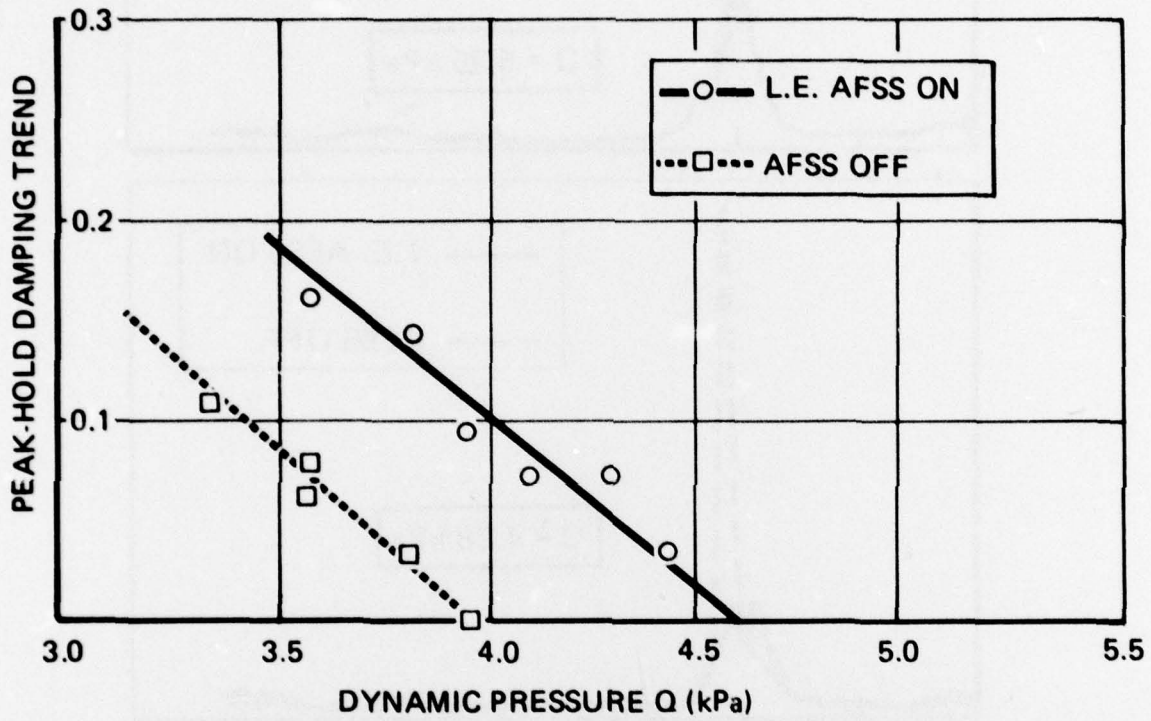


FIGURE 14. DAMPING TREND FOR CONFIGURATION (B),  
LEADING EDGE SYSTEM  $M = 0.80$

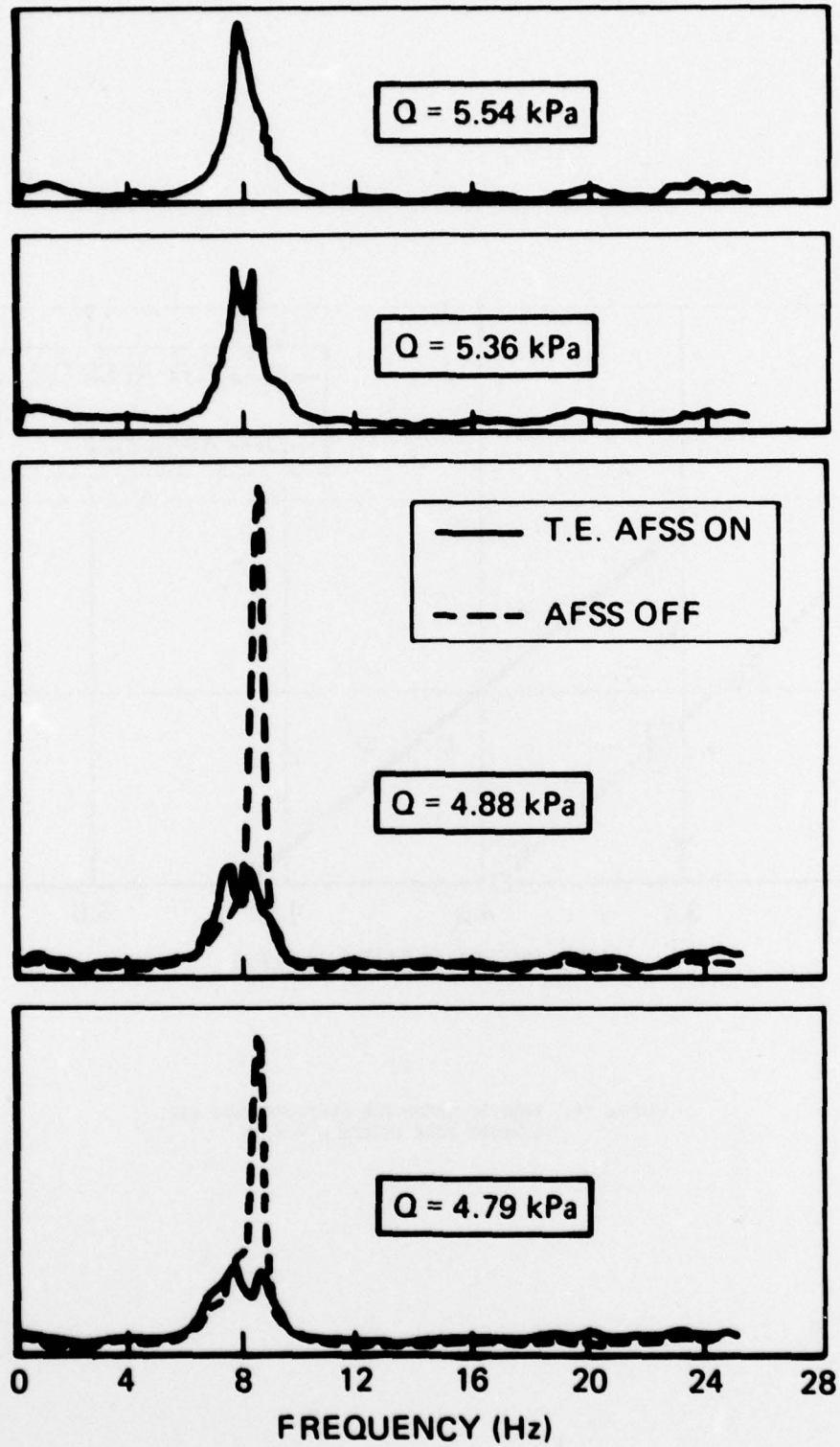


FIGURE 15. PEAK-HOLD SPECTRA OF WING ROOT TORSION MOMENT FOR CONFIGURATION (C) WITH LEADING EDGE CONTROL,  $M = 0.60$ . PROJECTED FLUTTER DYNAMIC PRESSURE  $Q = 5.10$  kPa

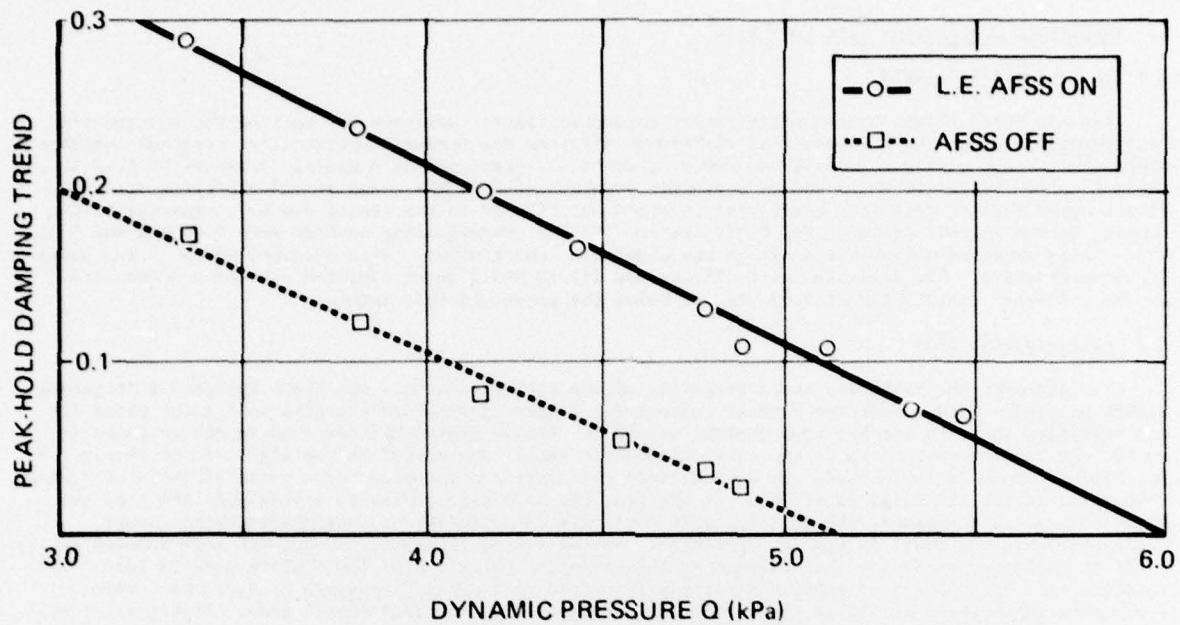


FIGURE 16. DAMPING TREND FOR CONFIGURATION (C),  
M = 0.60 LEADING EDGE SYSTEM

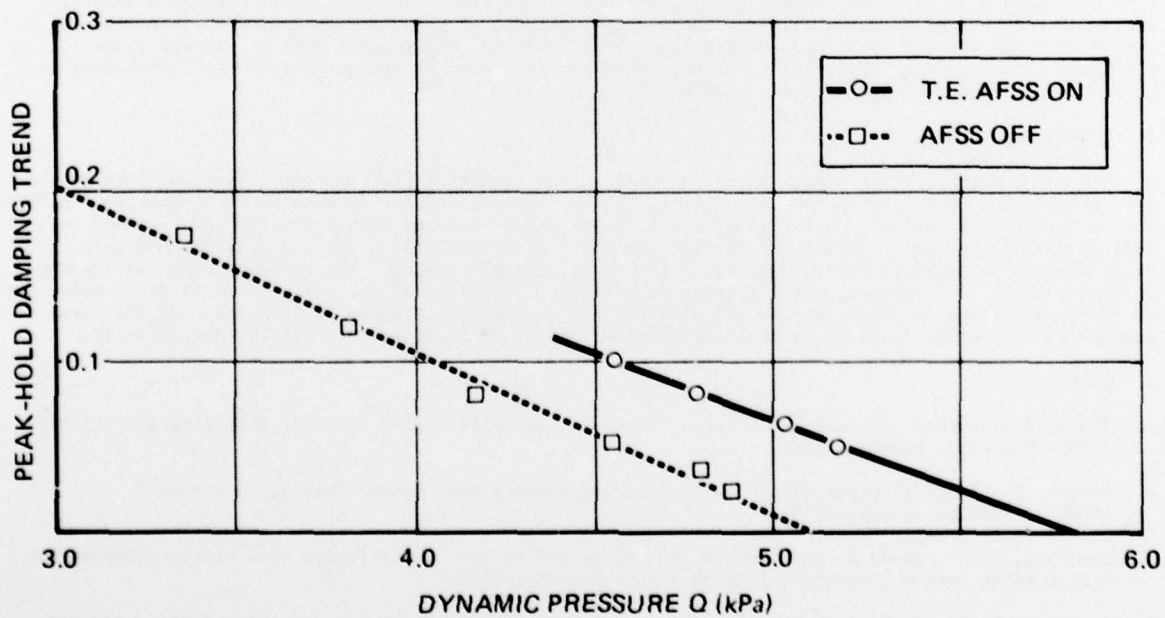


FIGURE 17. DAMPING TREND FOR CONFIGURATION (C),  
M = 0.60 TRAILING EDGE SYSTEM



predictions that, as a general rule, the flutter suppression loop required increasing phase lag with increasing Mach number. The analysis indicated that, in some cases, scheduling of the loop gain would be beneficial to maximize system damping at the subcritical dynamic pressures and to stabilize structural modes adjacent to the flutter mode. Further testing is required to investigate transonic effects and improvements of the control laws.

## 6. ANALYTICAL CORRELATION WITH TEST DATA

### 6.1 Analysis without AFSS

The Air Force Flight Dynamics Laboratory conducted flutter analyses for each of the unaugmented configurations using the FOP module of the FASTOP (Flutter and Strength Optimization Program) computer program<sup>(12)</sup>. For configuration (A) at  $M=0.8$ , flutter was predicted at a dynamic pressure of 6.42 kPa using computed vibration modes and at a dynamic pressure of 6.56 kPa using ground vibration test data. It was noted earlier that this configuration would not flutter in the tunnel due to unexpectedly high damping in the support system. For Configuration (B) the corresponding numbers were 3.64 kPa and 4.21 kPa. Using computed modes, the analysis was about 10% conservative. With measured modes it was about 4% unconservative. The analysis for Configuration (C) at  $M=0.6$  using computed vibration modes, predicted a flutter instability at 4.93 kPa, 2% below the projected test point.

### 6.2 Analysis with AFSS

To determine the stability characteristics of the augmented model, the AFFDL employed a frequency domain procedure with a modified Nyquist criterion. Figure 18 presents a series of Nyquist plots for configuration (B) with leading edge control at  $M=0.8$ . At low dynamic pressure where the response is small, the loop corresponding to the critical mode is small and located to the right of the origin. As the flutter speed is approached, the Nyquist loop gets larger and approaches a curve of infinite radius that turns in the clockwise direction. At flutter, the loop degenerates to a straight line. As the flutter speed is surpassed, the critical mode encircles the origin in a counter-clockwise manner indicating that the model is stable. For higher speeds (above flutter), the Nyquist loop becomes smaller until it no longer encircles the origin. At this point, suppression of the flutter mode is lost. For configuration (B), loss of flutter control was predicted at a dynamic pressure of 5.27 kPa. This represents an increase of 31% in flutter dynamic pressure over the unaugmented case. Experimental results at this Mach number indicated a projected increase of 15% using the peak-hold trend and a projected increase of 23% using the estimated damping ratios presented in Table 2.

The analyses for the augmented configuration (A) at  $M=0.8$  showed that the critical dynamic pressure could be increased by about 33% using either the leading edge or the trailing edge surface. Since this configuration was stable in the tunnel, it is difficult to make a meaningful comparison. For the augmented configuration (C) with leading edge control the analysis at  $M=0.6$  showed good stability characteristics up to dynamic pressures exceeding 9.58 kPa which is 48% above the unaugmented case. The test results, however, show a projected improvement of only 17%.

In general, control surface aerodynamic force and moment coefficients predicted by theory are high when compared to experimental data. Since experimental information on this model regarding control surface aerodynamics was not available, there was no attempt at this time to reduce the magnitude of the control surface aerodynamics. Unmodified control surface aerodynamics tend to predict a more efficient active flutter suppression system. This may be a partial explanation of the differences obtained between the analysis and test results.

## 7. CONCLUDING REMARKS

Although many problems remain to be solved in order to make a flutter control system truly adaptive, the present test program has demonstrated that active suppression of wing/store flutter is feasible for practical application. As far as known, this was the first time that a leading edge surface was used as the single active device for flutter control. Both the leading and the trailing edge surfaces were used independently to suppress a single flutter mode. There are several items that remain as future tasks. At present, the Air Force is reviewing plans to use the existing model for demonstration of improved control laws and various adaptive control schemes for flutter suppression. Another item considered for future testing, is the combined application of leading and trailing edge controls.

## 8. REFERENCES

1. The Boeing Company and Honeywell, Inc., "Aircraft Load Alleviation and Mode Stabilization (LAMS)", AFFDL-TR-68-158, December 1968.
2. Severt, D. F., "Development of Active Flutter Suppression Wind Tunnel Testing Technology", AFFDL-TR-74-126, January 1975.
3. Sandford, M. C., Abel, I. and Gray, D. L., "Development and Demonstration of a Flutter-Suppression System Using Active Controls", NASA TR R-450, December 1975.
4. Triplett, W. E., Kappus, H. P. F., and Landy, R. J., "Active Flutter Suppression Systems for Military Aircraft - A Feasibility Study", AFFDL-TR-72-116, February 1973.
5. Triplett, W. E., Landy, R. J., and Irwin, D. W., "Preliminary Design of Active Wing/Store Flutter Suppression Systems for Military Aircraft", AFFDL-TR-74-67, August 1974.
6. Sensburg, O., Hönlinger, H., and Kühn, M., "Active Control of Empennage Flutter", AGARD-CP-175, April 1975.

7. Destuynder, R., "Essai En Soufflerie D'un Suppresseur De Flottement Sur Une Aile Droite", AGARD-CP-175, April 1975.
8. Turner, M. R., "Active Flutter Suppression", AGARD-CP-175, April 1975.
9. Landahl, M. T., "Graphical Technique for Analyzing Marginally Stable Dynamic Systems", Journal of Aircraft, Vol. 1, No. 5, 1964.
10. Winther, B. A., "A Study on a Flutter Suppression System for the Northrop YF-17", Northrop Report NOR 74-64, July 1974.
11. Arthurs, T. D., Tye, R. R., and Winther, B. A., "Aeroelastic Airframe Transfer Function Synthesis". Presented at the AIAA/ASME/SAE Conference in May 1976.
12. Hammond, C. E. and Doggett, Jr., R. V., "Determination of Subcritical Damping by Moving-Block/Randomec Applications". Presented at the NASA Symposium on Flutter Testing Techniques, October 1975.
13. Wilkinson, K. et al, "An Automated Procedure for Flutter and Strength Analysis and Optimization of Aerospace Vehicles", AFFDL-TR-75-137, Volumes I and II, December 1975.

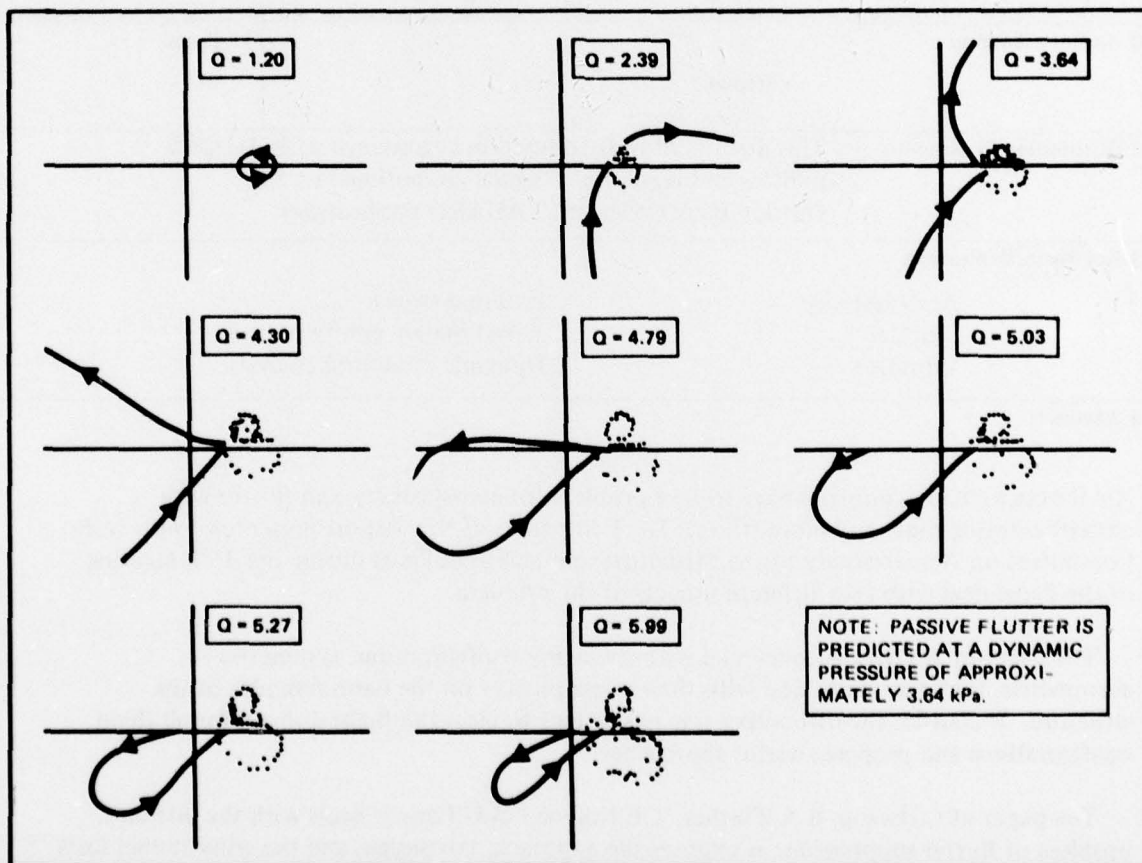


FIGURE 18. MODIFIED NYQUIST PLOTS FOR CONFIGURATION (B), LEADING EDGE SYSTEM  $M = 0.8$

**REPORT DOCUMENTATION PAGE**

<b>1. Recipient's Reference</b>	<b>2. Originator's Reference</b>	<b>3. Further Reference</b>	<b>4. Security Classification of Document</b>						
	AGARD-R-668	ISBN 92-835-1290-1	UNCLASSIFIED						
<b>5. Originator</b>	Advisory Group for Aerospace Research and Development North Atlantic Treaty Organization 7 rue Ancelle, 92200 Neuilly sur Seine, France								
<b>6. Title</b>	CONSIDERATIONS ON WING STORES FLUTTER – Asymmetry – Flutter Suppression								
<b>7. Presented at</b>	the 46th Structures and Materials Panel Meeting, held at Aalborg, Denmark, 10–14 April 1978.								
<b>8. Author(s)</b>	Various		<b>9. Date</b> July 1978						
<b>10. Author's Address</b>	Various		<b>11. Pages</b> 42						
<b>12. Distribution Statement</b>	This document is distributed in accordance with AGARD policies and regulations, which are outlined on the Outside Back Cover of all AGARD publications.								
<b>13. Keywords/Descriptors</b>	<table border="0"> <tr> <td>Aeroelasticity</td> <td>External stores</td> </tr> <tr> <td>Flutter</td> <td>Aerodynamic configurations</td> </tr> <tr> <td>Vibration</td> <td>Dynamic structural analysis</td> </tr> </table>			Aeroelasticity	External stores	Flutter	Aerodynamic configurations	Vibration	Dynamic structural analysis
Aeroelasticity	External stores								
Flutter	Aerodynamic configurations								
Vibration	Dynamic structural analysis								
<b>14. Abstract</b>	<p>Air Forces in many countries have to face problems of aeroelasticity and flutter with aircraft carrying more and more stores. The two papers of this Report presented to the Sub-Committee on Aeroelasticity of the Structures and Materials Panel during the 46th Meeting of the Panel deal with two different aspects of the problem.</p> <p>– The paper of A.Lotze is concerned with the many configurations, symmetric or asymmetric, that may occur and with their consequences on the natural modes of the structure. It clarifies the difficulties one has to face to clear the flight domain for all flight configurations and proposes useful approaches.</p> <p>– The paper of C.Hwang, B.A.Winther, T.E.Noll and M.G.Farmer deals with the difficult problem of flutter suppression; it exposes the approach, the design, and the wind tunnel tests of the model of a fighter, carrying stores and equipped with a flutter suppression device.</p> <p>The two papers are of great interest to aeroelasticians and may give useful help to the designer.</p>								

<p>AGARD Report No.668 Advisory Group for Aerospace Research and Development, NATO CONSIDERATIONS ON WING STORES FLUTTER - Asymmetry - Flutter Suppression Published July 1978 42 pages</p> <p>Air Forces in many countries have to face problems of aeroelasticity and flutter with aircraft carrying more and more stores. The two papers of this Report presented to the Sub-Committee on Aeroelasticity of the Structures and Materials Panel during the 46th Meeting of the Panel deal with two different aspects of the problem.</p> <p>P.T.O.</p>	<p>AGARD-R-668</p> <p>Aeroelasticity Flutter Vibration External stores Aerodynamic configurations Dynamic structure analysis</p>	<p>AGARD Report No.668 Advisory Group for Aerospace Research and Development, NATO CONSIDERATIONS ON WING STORES FLUTTER - Asymmetry - Flutter Suppression Published July 1978 42 pages</p> <p>Air Forces in many countries have to face problems of aeroelasticity and flutter with aircraft carrying more and more stores. The two papers of this Report presented to the Sub-Committee on Aeroelasticity of the Structures and Materials Panel during the 46th Meeting of the Panel deal with two different aspects of the problem.</p> <p>P.T.O.</p>	<p>AGARD-R-668</p> <p>Aeroelasticity Flutter Vibration External stores Aerodynamic configurations Dynamic structure analysis</p>
<p>AGARD Report No.668 Advisory Group for Aerospace Research and Development, NATO CONSIDERATIONS ON WING STORES FLUTTER - Asymmetry - Flutter Suppression Published July 1978 42 pages</p> <p>Air Forces in many countries have to face problems of aeroelasticity and flutter with aircraft carrying more and more stores. The two papers of this Report presented to the Sub-Committee on Aeroelasticity of the Structures and Materials Panel during the 46th Meeting of the Panel deal with two different aspects of the problem.</p> <p>P.T.O.</p>	<p>AGARD-R-668</p> <p>Aeroelasticity Flutter Vibration External stores Aerodynamic configurations Dynamic structure analysis</p>	<p>AGARD Report No.668 Advisory Group for Aerospace Research and Development, NATO CONSIDERATIONS ON WING STORES FLUTTER - Asymmetry - Flutter Suppression Published July 1978 42 pages</p> <p>Air Forces in many countries have to face problems of aeroelasticity and flutter with aircraft carrying more and more stores. The two papers of this Report presented to the Sub-Committee on Aeroelasticity of the Structures and Materials Panel during the 46th Meeting of the Panel deal with two different aspects of the problem.</p> <p>P.T.O.</p>	<p>AGARD-R-668</p> <p>Aeroelasticity Flutter Vibration External stores Aerodynamic configurations Dynamic structure analysis</p>

<p>- The paper of A.Lotze is concerned with the many configurations, symmetric or asymmetric, that may occur and with their consequences on the natural modes of the structure. It clarifies the difficulties one has to face to clear the flight domain for all flight configurations and proposes useful approaches.</p> <p>- The paper of C.Hwang, B.A.Winther, T.E.Noll and M.G.Farmer deals with the difficult problem of flutter suppression; it exposes the approach, the design, and the wind tunnel test of the model of a fighter, carrying stores and equipped with a flutter suppression device.</p> <p>The two papers are of great interest to aeroelasticians and may given useful help to the designer.</p> <p>These papers were presented at the 46th Structures and Materials Panel Meeting, held at Aalborg, Denmark, 10-14 April 1978.</p> <p>ISBN 92-835-1290-1</p>	<p>- The paper of A.Lotze is concerned with the many configurations, symmetric or asymmetric, that may occur and with their consequences on the natural modes of the structure. It clarifies the difficulties one has to face to clear the flight domain for all flight configurations and proposes useful approaches.</p> <p>- The paper of C.Hwang, B.A.Winther, T.E.Noll and M.G.Farmer deals with the difficult problem of flutter suppression; it exposes the approach, the design, and the wind tunnel test of the model of a fighter, carrying stores and equipped with a flutter suppression device.</p> <p>The two papers are of great interest to aeroelasticians and may given useful help to the designer.</p> <p>These papers were presented at the 46th Structures and Materials Panel Meeting, held at Aalborg, Denmark, 10-14 April 1978.</p> <p>ISBN 92-835-1290-1</p>
<p>- The paper of A.Lotze is concerned with the many configurations, symmetric or asymmetric, that may occur and with their consequences on the natural modes of the structure. It clarifies the difficulties one has to face to clear the flight domain for all flight configurations and proposes useful approaches.</p> <p>- The paper of C.Hwang, B.A.Winther, T.E.Noll and M.G.Farmer deals with the difficult problem of flutter suppression; it exposes the approach, the design, and the wind tunnel test of the model of a fighter, carrying stores and equipped with a flutter suppression device.</p> <p>The two papers are of great interest to aeroelasticians and may given useful help to the designer.</p> <p>These papers were presented at the 46th Structures and Materials Panel Meeting, held at Aalborg, Denmark, 10-14 April 1978.</p> <p>ISBN 92-835-1290-1</p>	<p>- The paper of A.Lotze is concerned with the many configurations, symmetric or asymmetric, that may occur and with their consequences on the natural modes of the structure. It clarifies the difficulties one has to face to clear the flight domain for all flight configurations and proposes useful approaches.</p> <p>- The paper of C.Hwang, B.A.Winther, T.E.Noll and M.G.Farmer deals with the difficult problem of flutter suppression; it exposes the approach, the design, and the wind tunnel test of the model of a fighter, carrying stores and equipped with a flutter suppression device.</p> <p>The two papers are of great interest to aeroelasticians and may given useful help to the designer.</p> <p>These papers were presented at the 46th Structures and Materials Panel Meeting, held at Aalborg, Denmark, 10-14 April 1978.</p> <p>ISBN 92-835-1290-1</p>